

diflomotecan,<sup>27</sup> rosuvastatin,<sup>28</sup> and gefitinib.<sup>30,31</sup> Available data indicate that the *ABCG2-A* allele was associated with remarkably decreased BCRP expression compared with WT cells and human placental samples.<sup>33,34</sup> Since BCRP is highly expressed at the apical membrane of enterocytes and hepatocytes,<sup>22,25</sup> impaired transport activity caused by the *ABCG2-A* allele may lead to increased absorption at the intestinal epithelium, and/or to decreased biliary excretion of substrates, thereby resulting in elevated plasma concentrations in subjects with *ABCG2-A* allele(s) (Figure 1). Thus, the raised AUC of SASP in *ABCG2-A* subjects may be due to increased oral availability (F) and/or decreased hepatic clearance. Nevertheless, we have recently demonstrated no significant effect of the *ABCG2 421C>A* polymorphism on the pharmacokinetics of pitavastatin, a good substrate for BCRP, suggesting that the pharmacogenomic effect of the *ABCG2* polymorphism appeared to depend on the substrate.<sup>32</sup>

The raised AUC of SASP in *ABCG2-A* subjects is in accord with the findings in a BCRP<sup>-/-</sup> mouse study that, after oral administration, AUC of SASP in BCRP<sup>-/-</sup> was ~111-fold higher than that in FVB-WT mice.<sup>29</sup> Interestingly, after intravenous administration, the AUC in BCRP<sup>-/-</sup> was 13-fold higher than that in FVB-WT mice. The absolute F for SASP varied between 4 and 37% in FVB-WT and BCRP<sup>-/-</sup> mice, respectively. These results show that BCRP (*Abcg2*) plays a major role in the intestinal absorption of SASP in mice.<sup>29</sup> In this study, we could not determine F due to the lack of an intravenous formulation of SASP, making it difficult to describe how extent *ABCG2* polymorphism influences the intestinal absorption, intestinal secretion, and/or the biliary excretion of SASP. However, since total urinary recovery (4.5% of the dose) and biliary recovery (2.5% of the dose, about half the value of urinary recovery) of SASP have been reported to be very low in humans, the contribution of BCRP to the biliary excretion of SASP is thought to be small.<sup>35,36</sup>

In contrast to SASP, mean AUC<sub>0-48</sub> and C<sub>max</sub> values of SP tended to be lower in *ABCG2-A/A* compared with those in *ABCG2-C/C* subjects, except for SA subjects (Table 3). After oral administration, most SASP travels down the small intestine to the lower intestinal tract (i.e., colon and cecum) where its diazo-bond is cleaved by colonic bacteria with the liberation of SP and 5-ASA (Figure 1).<sup>7</sup> SP is almost totally absorbed from the colon and cecum, and then metabolized into AcSP by NAT2, predominantly in the liver.<sup>7-10</sup> The amount of SASP in the lower intestinal tract may be lower in *ABCG2-A/A* subjects than in *ABCG2-C/C* subjects due to high BCRP expression on the brush border of the small intestinal enterocytes in *ABCG2-C/C* subjects (i.e., reduction in the intestinal secretion of SASP into the gut lumen in *ABCG2-A/A* subjects), leading to lower conversion in the distal intestine to SP in *ABCG2-A/A* subjects. Individual variability of bacterial azo reductase as a result of gastrointestinal disease(s) and/or antibiotics therapy may alter the production of SP; however, all subjects were healthy volunteers who had not taken antibiotics for at least 2 months before or during this investigation. Moreover, similar findings were observed in previous BCRP<sup>-/-</sup> and WT mice.<sup>29</sup>

The mean  $t_{1/2}$  and C<sub>max</sub> of SP were also significantly different among three *ABCG2-C/A*-matched NAT2 genotyping subjects;

the order was SA > IA > RA (Table 3). Generally, C<sub>max</sub> is determined by dose (the amount of SP in the colon and cecum in this case), K<sub>e</sub>, and K<sub>a</sub> (absorption rate constant). Since the dose can be assumed to be similar among the same *ABCG2* genotyping groups, and since K<sub>a</sub> was comparable among these three *ABCG2-C/A*-matched NAT2 genotyping subjects (data not shown), C<sub>max</sub> may be dependent on the NAT2 genotyping-dependent K<sub>e</sub> value.

Interestingly, no changes in the pharmacokinetics of SP were recognized in SA subjects. The reason for the discrepancy with the data obtained from RA and IA subjects is presently unclear.

In this study, we also genotyped *ABCG2 34G>A*, another relatively frequent polymorphism among the Japanese population,<sup>33</sup> and similar phenotyping-genotyping analysis was attempted. The allelic frequency of 34A in our subjects was 14.9% (26 subjects were 34G/G and 11 were 34G/A). The mean AUC<sub>0-48</sub> and CL<sub>total</sub>/F of SASP in *ABCG2-34G/G421C/C* (n = 5) and *ABCG2-34G/A421C/C* (n = 7) were 170 ± 85 and 173 ± 92 µg h/ml, and 14.3 ± 7.2 and 13.2 ± 5.1 l/h, respectively. Similar trends were observed in the pharmacokinetic parameters of three compounds with other genotyping patterns. These results suggest that *ABCG2 34G>A* does not play an important role in the overall pharmacokinetics of SASP; however, since we had no homozygote for the 34A allele in this study, further study is necessary to confirm these observations.

The mean AUC ratio of AcSP to SP (AUC<sub>AcSP</sub>/AUC<sub>SP</sub>) and 48-h cumulative urinary excretion of AcSP were significantly higher in RA than in SA subjects (Table 5). We confirmed previous studies that NAT2 genotypes are well-correlated with plasma concentrations and urinary excretions of SP and AcSP.<sup>7,17,37</sup> In view of the pharmacodynamics, the occurrence of certain adverse events of SASP has been speculated to be dependent on NAT2 genotyping; higher incidences of nausea/vomiting and hepatic disorders were reported in SA subjects.<sup>17-19</sup>

Since overall pharmacokinetic profiles of SASP would be determined not only by NAT2 but also by *ABCG2* genotyping results, it is of interest whether the risk of SASP-induced adverse events and the clinical efficacy of SASP can be partially attributed to the *ABCG2*. Until now, the action mechanism of SASP in ulcerative colitis and Crohn's disease has not been well understood. The most prevalent scenario is that SASP serves as a vehicle to deliver SP and 5-ASA to the colon and cecum in higher concentrations than can be achieved by oral administration of these metabolites alone.<sup>7,8,36,38,39</sup> If these hypotheses are correct, subjects with the *ABCG2-A* allele are expected to exhibit reduced clinical efficacy owing to lower SASP exposure in the lower intestinal tract (which, in turn, may be associated with lower SP and 5-ASA formations in this tract), despite high plasma concentrations and AUC of SASP. Similar to ulcerative colitis and Crohn's disease, questions still exist as to whether SASP itself or its metabolites, SP and 5-ASA, are responsible for specific antirheumatic effects of SASP; however, there is evidence that SP is also the active moiety of SASP in rheumatoid arthritis.<sup>5,6</sup> The effect of *ABCG2* gene polymorphism on the clinical efficacy and adverse events of SASP will be the subject of further investigation.

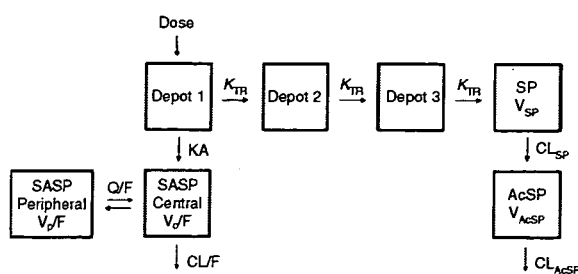


**Figure 5** Scheme of the pharmacokinetic compartment model for simultaneous description of sulfasalazine (SASP), sulfapyridine (SP), and *N*-acetylsulfapyridine (AcSP) plasma concentrations.

Previous studies demonstrated that SASP concentrations in serum and urine did not differ before and after colectomy and ileostomy, while the concentration of SP and its metabolites decreased markedly in patients with inflammatory bowel disease.<sup>7,36</sup> Similarly, in two patients with transverse colostomy, serum and urine concentrations of SASP did not differ from those of patients with ileostomy.<sup>36</sup> Although BCRP has been reported to be expressed in the epithelium of the colon,<sup>21–25</sup> these observations suggest that the upper intestinal tract (i.e., small intestine) is the major site of SASP absorption.<sup>7</sup> Thus, in order to detect the effect of BCRP on the pharmacokinetic profiles of SASP more precisely, we used a conventional tablet as the test drug in this study. Whether *ABCG2* genotype-dependent changes in the pharmacokinetics of SASP occur with the enteric-coated formulation is of interest as well.

As shown in Figures 3 and 4, it is notable that NONMEM analysis with Erlang's distribution model gave good descriptions of all three compounds, indicating that the present structural model (Figure 5) is suitable to describe the three compounds simultaneously. A significant contribution of *ABCG2* and *NAT2* polymorphisms to *Fr*, *K<sub>a</sub>*, and  $CL_{SASP}/F$ , and  $CL_{SP}$ , respectively, was detected. The relative value of *Fr* in *ABCG2*-*C/C*, *C/A*, and *A/A* subjects was 1:1.7:2.1, indicating that the bioavailability of SASP is higher in subjects with at least one *ABCG2*-*A* allele as compared with that in *ABCG2*-*C/C* subjects. A similar influence was previously suggested for various substrate drugs.<sup>26–28</sup> Of note, relative  $CL_{SASP}/F$  in *ABCG2*-*C/C*, *C/A*, and *A/A* subjects was 1:0.84:0.84. These results suggest that *CL* in subjects with at least the *ABCG2*-*A* allele was 16% lower than that in *ABCG2*-*C/C* subjects.

In conclusion, this study shows that the overall pharmacokinetics of SASP are highly dependent on interplay with *NAT2* and BCRP; polymorphisms in both genes are associated with individual variability in pharmacokinetic profiles. In spite of the small sample studied here, it is suggested that SASP is a candidate probe for BCRP in humans and that BCRP restricts the oral absorption and/or biliary excretion of substrate drugs. Obviously, the number of subjects is a drawback of our study. Since the frequencies of *SA* and *ABCG2*-*A/A* types are low in Japanese,<sup>15,17,33</sup> the study subjects were recruited from a population of >100 male Japanese volunteers whose *NAT2* and *ABCG2* genotypes were prescreened. Nevertheless, it is clear that the current observation warrants confirmation and further

investigation of SASP and other substrates for BCRP in large populations involving different ethnic groups.

## METHODS

**Subjects and genotyping of *ABCG2* and *NAT2*.** This study was approved by the Ethics Review Boards of Kyushu University and Kyushu Pharmacology Research Clinic, and written informed consent was obtained from all participants before the study. Thirty-seven unrelated healthy male volunteers (age: 20–24 years; weight: 49.5–79.7 kg) were selected from our study panels based on their genotyping for *ABCG2* and *NAT2*. They were recruited from a population of >100 male Japanese volunteers whose genotypes were prescreened after written informed consent was obtained. Each subject was physically normal and had no antecedent history of significant medical illness or hypersensitivity to any drugs, and each had a body mass index between 17.6 and 25.5 kg/m<sup>2</sup>. Their health status was judged to be normal on the basis of a physical examination with a screening of blood chemistry, complete blood count, urinalysis, electrocardiogram, and chest X-ray before the study. None had taken any drugs for at least 1 week before the study.

Genomic DNA was isolated from blood samples using the Toyobo blood kit on a Toyobo HMX-2000 robot (Toyobo, Osaka, Japan). In the *ABCG2* gene, 421C>A variant was identified using TaqMan primers and probes for the Sequence Detection System (ABI PRISM 7000; Applied Biosystems, Foster, CA). The following primers and probes were developed: forward primer, GGGCACTCTGACGGTGAGA; reverse primer, CATAGTTGTTGCAAGCCGAAGAG; probe 1 (C allele), VIC-TGAGAAGCTGTAAGTTT; probe 2 (A allele), FAM-TGCTGA GAACCTTAAG. In the *NAT2* gene, we identified *NAT2*\*5B, \*6A, and \*7B mutant alleles using commercially available TaqMan Genotyping Assay (Drug Metabolism) kits (Applied Biosystems). All subjects were classified into three groups according to their *NAT2* genotypes: RA genotype (RA, a homozygote for *NAT2*\*4), intermediate (IA, a heterozygote for mutant alleles) and SA genotypes (SA, a combination of mutant alleles). As only four alleles (*NAT2*\*4, \*5B, \*6A, and \*7B) have been reported to date in Japanese subjects,<sup>12</sup> identification of these three variants is sufficient to define almost all *NAT2* alleles in a homozygous Japanese population.<sup>13,17</sup> All real-time polymerase chain reaction assays were carried out according to the manufacturer's instructions.

In this study, we selected the following genotypings with regard to the combination of two genes of interest: RA-*ABCG2*-*C/C* (i.e., a homozygote for *ABCG2*-*C* allele and RA genotype, *n* = 5), RA-*C/A* (*n* = 5), RA-*A/A* (*n* = 3), IA-*C/C* (*n* = 5), IA-*C/A* (*n* = 5), IA-*A/A* (*n* = 6), SA-*C/C* (*n* = 2), and SA-*C/A* (*n* = 6).

**Study protocol.** The participants came to the clinic after an overnight fast. They were required to abstain from alcohol for 2 days before drug administration and during the period of hospitalization, and were served standard meals on the study day. Each subject received a single oral dose of 2,000 mg of SASP (Salazopyrin conventional tablet, Pfizer, Tokyo, Japan) with 200 ml of water. Food was given 4 h after the ingestion of SASP. Venous blood samples (5 ml each) to determine SASP, SP, and AcSP concentrations were obtained just before and 0.5, 1, 2, 3, 4, 6, 9, 12, 24, 36, and 48 h after dosing. Plasma samples were immediately separated after centrifugation. Urine samples (20 ml each) were collected cumulatively in two fractions: 0 to 24 and 24 to 48 h. The amount and pH of urine were measured. Both plasma and urine samples were stored at -20 °C until analyzed.

**Quantification of SASP, SP, and AcSP.** The concentrations of SASP, SP, and AcSP in plasma and urine were measured by high-performance liquid chromatography as described previously.<sup>37,40,41</sup> High-performance liquid chromatography was equipped with a system controller (SCL-10A, Shimadzu, Kyoto, Japan), a variable wavelength ultraviolet detector (SPD-10A, Shimadzu) adjusted to 254 nm for SASP, 260 nm for SP and AcSP, and a data processor (C-R7Ae plus, Shimadzu). The stationary

phase was a reversed phase Chemcobond 5-ODS-H column (4.6 mm i.d. × 250 mm, particle size 5 μm, Chemco, Osaka, Japan).

### Pharmacokinetic and statistical analysis

**Non compartmental analysis.**  $C_{max}$  and  $T_{max}$  were obtained directly from the data. The  $AUC_{0-48}$  was calculated by the linear trapezoidal rule. We calculated the apparent oral clearance ( $CL_{tot}/F$ ) as follows:  $CL_{tot}/F = \text{Dose}/AUC_{0-48}$ . The  $K_e$  was estimated using least-squares regression analysis from the terminal postdistribution phase of the concentration–time curve.  $CL_r$  was calculated by  $CL_r = Ae_{0-48}/AUC_{0-48}$ , where  $Ae_{0-48}$  represents the amount of compounds excreted in urine.

**Nonmem.** Simultaneous modeling of SASP, SP, and AcSP with regard to the polymorphism of *ABCG2* and *NAT2* genes was assessed by the nonlinear mixed-effects modeling approach with the software package NONMEM, version V, level 1.1 (NONMEM Project Group, University of California at San Francisco).<sup>42</sup> Throughout the analysis, the first-order method was used as the estimation method. The pharmacokinetic model for all three compounds is shown in Figure 5. The two-compartment model with lag time assumed that first-order absorption was applied for the description of SASP disposition, and the one-compartment model was applied for SP and AcSP dispositions. To describe the absorption phase of SP, Erlang's distribution model was used.<sup>43,44</sup> Erlang's distribution is the analytical solution for a linear chain of  $n$  identical compartments placed upstream of the central compartment and connected by an identical transfer rate constant  $K_{TR}$ , the transfer constant between two sequential delay compartments.<sup>43,44</sup> In the present model, the number of serial compartments  $n$  was set to 3 for all subjects, based on the objective function value and predictive performance. Interindividual variability of all parameters was modeled as the exponential error model. As the intraindividual variability model, the exponential error model was selected for SASP and the combined additive and exponential error model was used for SP and AcSP.

The contribution of body weight, body surface area, and candidates of physiological covariate to CL and V of the three compounds was tested.

The effect of the *ABCG2* 421C>A genotype on  $K_a$ ,  $CL/F$ , and  $V/F$  was assessed with the following equation:

$$Pi = TVPi \times \theta^{ABCG2421C/A} \times \theta^{ABCG2421A/A}$$

where  $Pi$  is the individual value and  $TVPi$  is the population average value for *ABCG2*-C/C (i.e., a homozygote for the WT allele) subjects.

The effect of the *NAT2* genotype on CL of SP was assessed with the following equation:

$$Pi = TVPi \times \theta^{NAT2IA} \times \theta^{NAT2SA}$$

where  $TVPi$  is the population average value for RA subjects.

Forward addition and backward exclusion methods were used to build the final model. The significance of the genotype effect was assessed by comparing the objective functions ( $-2 \log$  likelihood) for different models, assuming  $\chi^2$  distribution of their difference, and by assessing the 95% confidence interval for estimated values.

**Statistical analysis.** Statistical differences among the data for each group were determined by ANOVA, followed by Fisher's least significant difference test.  $P < 0.05$  was considered statistically significant.

### ACKNOWLEDGMENTS

This study was supported by a Health and Labour Sciences Research Grant from the Ministry of Health, Labour and Welfare for Research on Advanced Medical Technology.

### CONFLICT OF INTEREST

The authors declared no conflict of interest.

© 2008 American Society for Clinical Pharmacology and Therapeutics

1. Peppercorn, M.A. Sulfasalazine. Pharmacology, clinical use, toxicity, and related new drug development. *Ann. Intern. Med.* **101**, 377–386 (1984).

2. Rains, C.P., Noble, S. & Faulds, D. Sulfasalazine: A review of its pharmacological properties and therapeutic efficacy in the treatment of rheumatoid arthritis. *Drugs* **50**, 137–156 (1995).
3. Houston, J.B., Day, J. & Walker, J. Azo reduction of sulphasalazine in healthy volunteers. *Br. J. Clin. Pharmacol.* **14**, 395–398 (1982).
4. Peppercorn, M.A. & Goldman, P. The role of intestinal bacteria in the metabolism of salicylazosulphapyridine. *J. Pharmacol. Exp. Ther.* **181**, 555–562 (1972).
5. Bird, H.A. Sulphasalazine, sulphapyridine or 5-aminosalicylic acid—which is the active moiety in rheumatoid arthritis? *Br. J. Rheumatol.* **34** (suppl.2), 16–19 (1995).
6. Pullar, T., Hunter, J.A. & Capell, H.A. Which component of sulphasalazine is active in rheumatoid arthritis? *Br. Med. J.* **290**, 1535–1538 (1985).
7. Das, K.M. & Dubin, R. Clinical pharmacokinetics of sulphasalazine. *Clin. Pharmacokinet.* **1**, 406–425 (1976).
8. Das, K.M., Eastwood, M.A., McManus, J.P.A. & Sircus, W. The metabolism of salicylazosulphapyridine in ulcerative colitis I. The relationship between metabolites and the response to treatment in inpatients. *Gut* **14**, 631–636 (1973).
9. Das, K.M., Eastwood, M.A., McManus, J.P.A. & Sircus, W. The metabolism of salicylazosulphapyridine in ulcerative colitis II. The relationship between metabolites and the progress of the disease studied in outpatients. *Gut* **14**, 637–641 (1973).
10. Schroder, H. & Campbell, D.E. Absorption, metabolism, and excretion of salicylazosulphapyridine in man. *Clin. Pharmacol. Ther.* **13**, 539–551 (1972).
11. Matas, N., Thygesen, P., Stacey, M., Risch, A. & Sim, E. Mapping AAC1, AAC2 and AAC3, the genes for arylamine N-acetyltransferases, carcinogen metabolising enzymes on human chromosome 8p22, a region frequently deleted in tumours. *Cytogenet. Cell Genet.* **77**, 290–295 (1997).
12. Abe, M., Deguchi, T. & Suzuki, T. The structure and characteristics of a fourth allele of polymorphic N-acetyltransferase gene found in the Japanese population. *Biochem. Biophys. Res. Commun.* **191**, 811–816 (1993).
13. Deguchi, T., Mashimo, M. & Suzuki, T. Correlation between acetylator phenotypes and genotypes of polymorphic arylamine N-acetyltransferase in human liver. *J. Biol. Chem.* **265**, 12757–12760 (1990).
14. Parkin, D.P. et al. Trimodality of isoniazid elimination: phenotype and genotype in patients with tuberculosis. *Am. J. Respir. Crit. Care Med.* **155**, 1717–1722 (1997).
15. Okumura, K., Kita, T., Chikazawa, S., Komada, F., Iwakawa, S. & Tanigawara, Y. Genotyping of N-acetylation polymorphism and correlation with procainamide metabolism. *Clin. Pharmacol. Ther.* **61**, 509–517 (1997).
16. Human *NAT2* alleles. <http://louisville.edu/medschool/pharmacology/NAT2.html>
17. Tanigawara, Y. et al. N-acetyltransferase 2 genotype-related sulfapyridine acetylation and its adverse events. *Biol. Pharm. Bull.* **25**, 1058–1062 (2002).
18. Pounder, R.E., Craven, E.R., Henthorn, J.S. & Bannatyne, J.M. Red cell abnormalities associated with sulfasalazine maintenance therapy for ulcerative colitis. *Gut* **16**, 181–185 (1975).
19. Wadelius, M., Stjernberg, E., Wiholm, B.E. & Rane, A. Polymorphisms of *NAT2* in relation to sulphasalazine-induced agranulocytosis. *Pharmacogenetics* **10**, 35–41 (2000).
20. Machida, H. et al. Crohn's disease in Japanese is associated with a SNP-haplotype of N-acetyltransferase 2 gene. *World J. Gastroenterol.* **11**, 4833–4837 (2005).
21. Cervenak, J. et al. The role of the human *ABCG2* multidrug transporter and its variants in cancer therapy and toxicology. *Cancer Lett.* **234**, 62–72 (2006).
22. Maliepaard, M. et al. Subcellular localization and distribution of the breast cancer resistance protein transporter in normal human tissues. *Cancer Res.* **61**, 3458–3464 (2001).
23. Kruijtzter, C.M., Beijnen, J.H. & Schellens, J.H. Improvement of oral drug treatment by temporary inhibition of drug transporters and/or cytochrome P450 in the gastrointestinal tract and liver: an overview. *Oncologist* **7**, 516–530 (2002).
24. Taipalensuu, J. et al. Correlation of gene expression of ten drug efflux proteins of the ATP-binding cassette transporter family in normal human jejunum and in human intestinal epithelial Caco-2 cell monolayers. *J. Pharmacol. Exp. Ther.* **299**, 164–170 (2001).
25. Doyle, L.A. & Ross, D.D. Multidrug resistance mediated by the breast cancer resistance protein BCRP (*ABCG2*). *Oncogene* **22**, 7340–7358 (2003).
26. Sparreboom, A. et al. Effect of *ABCG2* genotype on the oral bioavailability of topotecan. *Cancer Biol. Ther.* **4**, 650–653 (2005).
27. Sparreboom, A. et al. Diflomotecan pharmacokinetics in relation to *ABCG2* 421C>A genotype. *Clin. Pharmacol. Ther.* **76**, 38–44 (2004).
28. Zhang, W. et al. Role of BCRP 421C>A polymorphism on rosvastatin pharmacokinetics in healthy Chinese males. *Clin. Chim. Acta.* **373**, 99–103 (2006).

29. Zaher, H., Khan, A.A., Palandra, J., Brayman, T.G., Yu, L. & Ware, J.A. Breast cancer resistance protein (Bcrp/abcg2) is a major determinant of sulfasalazine absorption and elimination in the mouse. *Mol. Pharm.* **3**, 55–61 (2006).
30. Li, J. *et al.* Association of variant ABCG2 and the pharmacokinetics of epidermal growth factor receptor tyrosine kinase inhibitors in cancer patients. *Cancer Biol. Ther.* **6**, 432–438 (2007).
31. Cusatis, G. *et al.* Pharmacogenetics of ABCG2 and adverse reactions to gefitinib. *J. Natl. Cancer Inst.* **98**, 1739–1742 (2006).
32. Ieiri, I. *et al.* SLCO1B1 (OATP1B1, an uptake transporter) and ABCG2 (BCRP, an efflux transporter) variant alleles and pharmacokinetics of pitavastatin in healthy volunteers. *Clin. Pharmacol. Ther.* **82**, 541–547 (2007).
33. Kobayashi, D. *et al.* Functional assessment of ABCG2 (BCRP) gene polymorphisms to protein expression in human placenta. *Drug Metab. Dispos.* **33**, 94–101 (2005).
34. Kondo, C. *et al.* Functional analysis of SNPs variants of BCRP/ABCG2. *Pharm. Res.* **21**, 1895–1903 (2004).
35. Azad Khan, A.K., Truelove, S.C. & Aronson, J.K. The disposition and metabolism of sulphasalazine (salicylazosulphapyridine) in man. *Br. J. Clin. Pharmacol.* **13**, 523–528 (1982).
36. Das, K.M., Eastwood, M.A., McManus, J.P.A. & Sircus, W. The role of the colon in the metabolism of salicylazosulphapyridine. *Scand. J. Gastroenterol.* **9**, 137–141 (1974).
37. Kita, T. *et al.* N-Acetyltransferase 2 genotype correlates with sulfasalazine pharmacokinetics after multiple dosing in healthy Japanese subjects. *Biol. Pharm. Bull.* **24**, 1176–1180 (2001).
38. Goldman, P. & Peppercorn, M.A. Drug therapy-sulfasalazine. *New Eng. J. Med.* **293**, 20–23 (1975).
39. Peppercorn, M.A. & Goldman, P. Distribution studies of salicylazosulphapyridine and its metabolites. *Gastroenterology* **64**, 240–245 (1973).
40. Show, P.N., Sivner, A.L., Aarons, L. & Houston, J.B. A rapid method for the simultaneous determination of the major metabolites of sulphasalazine in plasma. *J. Chromatogr.* **274**, 393–397 (1983).
41. Chungi, V.S., Rekhi, G.S. & Shargel, L. A simple and rapid liquid chromatographic method for the determination of major metabolites of sulfasalazine in biological fluids. *J. Pharm. Sci.* **78**, 235–238 (1989).
42. Beal, S.L. & Sheiner, L.B. NONMEM User's Guides. San Francisco, CA, NONMEM Project Group, University of California at San Francisco, San Francisco, CA (1998).
43. Djebli, N. *et al.* Sirolimus population pharmacokinetic/pharmacogenetic analysis and Bayesian modelling in kidney transplant recipients. *Clin. Pharmacokinet.* **45**, 1135–1148 (2006).
44. Saint-Marcoux, F. *et al.* Patient characteristics influencing ciclosporin pharmacokinetics and accurate Bayesian estimation of ciclosporin exposure in heart, lung and kidney transplant patients. *Clin. Pharmacokinet.* **45**, 905–922 (2006).

# *SLCO1B1* (OATP1B1, an Uptake Transporter) and *ABCG2* (BCRP, an Efflux Transporter) Variant Alleles and Pharmacokinetics of Pitavastatin in Healthy Volunteers

I Ieiri<sup>1</sup>, S Suwannakul<sup>1</sup>, K Maeda<sup>2</sup>, H Uchimaru<sup>3</sup>, K Hashimoto<sup>1</sup>, M Kimura<sup>3</sup>, H Fujino<sup>4</sup>, M Hirano<sup>4</sup>, H Kusuhara<sup>2</sup>, S Irie<sup>3</sup>, S Higuchi<sup>1</sup> and Y Sugiyama<sup>2</sup>

To investigate the contribution of genetic polymorphisms of *SLCO1B1* and *ABCG2* to the pharmacokinetics of a dual substrate, pitavastatin, 2 mg of pitavastatin was administered to 38 healthy volunteers and pharmacokinetic parameters were compared among the following groups: 421C/C\*1b/\*1b (group 1), 421C/C\*1b/\*15 (group 2), 421C/C\*15/\*15 and 421C/A\*15/\*15 (group 3), 421C/A\*1b/\*1b (group 4), 421A/A\*1b/\*1b (group 5), and 421C/A\*1b/\*15 (group 6). In *SLCO1B1*, pitavastatin area under plasma concentration–time curve from 0 to 24 h ( $AUC_{0-24}$ ) for groups 1, 2, and 3 was  $81.1 \pm 18.1$ ,  $144 \pm 32$ , and  $250 \pm 57$  ng h/ml, respectively, with significant differences among all three groups. In contrast to *SLCO1B1*,  $AUC_{0-24}$  in groups 1, 4, and 5 was  $81.1 \pm 18.1$ ,  $96.7 \pm 35.4$ , and  $78.2 \pm 8.2$  ng h/ml, respectively. Although the *SLCO1B1* polymorphism was found to have a significant effect on the pharmacokinetics of pitavastatin, a nonsynonymous *ABCG2* variant, 421C>A, did not appear to be associated with the altered pharmacokinetics of pitavastatin.

Pitavastatin is a highly potent inhibitor of 3-hydroxymethylglutaryl coenzyme A reductase and is used for the treatment of hypercholesterolemia.<sup>1</sup> In humans, pitavastatin is scarcely metabolized by the cytochrome P450 2C9,<sup>2,3</sup> and lactonization is another known metabolic pathway.<sup>4,5</sup> The lactone form can be reversibly converted to the parent drug.<sup>4</sup> Cumulative evidence has indicated that various active transport mechanisms are involved in its distribution and disposition kinetics. Pitavastatin is taken up efficiently from the circulation into hepatocytes by an organic anion-transporting polypeptide (OATP) 1B1 (formally known as OATP-C or OATP2, gene *SLCO1B1*), a sodium-independent bile-acid transporter expressed at the sinusoidal membrane of human hepatocytes responsible for the hepatocellular uptake of a variety of endogenous and foreign chemicals.<sup>6–8</sup> In addition to the uptake process, a recent study demonstrated that breast cancer resistance protein (BCRP, gene *ABCG2*) is involved in the biliary excretion of pitavastatin.<sup>9</sup> BCRP is expressed at the apical membrane in the placenta (trophoblast cells), liver (bile canalicular membrane of hepatocytes),

kidney, and intestine (enterocytes).<sup>10–13</sup> The biliary excretion clearance of pitavastatin in Bcrp1 (–/–) mice was 10 times lower than that in control mice;<sup>9</sup> thus, at least two drug transporters, OATP1B1 and BCRP, contribute to hepatic uptake and efflux of pitavastatin in humans.

A number of single nucleotide polymorphisms have been identified in *SLCO1B1* and some of these single nucleotide polymorphisms are associated with a significant change in the transporter activity of OATP1B1. Two commonly occurring single nucleotide polymorphisms, 388A>G (130Asn>Asp) and 521T>C (174Val>Ala), are found to cause a remarkable change in the disposition of OATP1B1 substrates such as statins (pravastatin<sup>14–17</sup> and pitavastatin<sup>18</sup>), fexofenadine,<sup>19</sup> and repaglinide.<sup>20</sup> Interestingly, most human studies have demonstrated that subjects with haplotypes *SLCO1B1*\*5, \*15, or \*17, all haplotypes harboring the 174Val>Ala variant, showed increased plasma levels of substrates as compared with subjects having the *SLCO1B1*\*1a (130Asn174Val) or \*1b (130Asp174Val) allele as homozygosity. Furthermore, recent studies reported that the

<sup>1</sup>Department of Clinical Pharmacokinetics, Graduate School of Pharmaceutical Sciences, Kyushu University, Fukuoka, Japan; <sup>2</sup>Department of Molecular Pharmacokinetics, Graduate School of Pharmaceutical Sciences, The University of Tokyo, Tokyo, Japan; <sup>3</sup>Kyushu Clinical Pharmacology Research Clinic, Fukuoka, Japan; <sup>4</sup>Tokyo New Drug Research Laboratories, Kowa Company Ltd., Tokyo, Japan. Correspondence: Y Sugiyama (sugiyama@mol.f.u-tokyo.ac.jp)

Received 19 October 2006; accepted 9 February 2007; published online 25 April 2007. doi:10.1038/sj.cpt.6100190

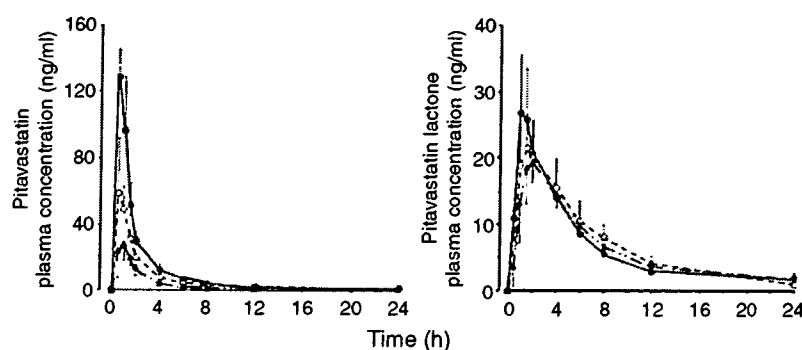


**Figure 1** Effect of *SLCO1B1* haplotype on pharmacokinetics of pitavastatin. Plasma concentration–time profiles of pitavastatin and pitavastatin lactone after oral administration of 2 mg pitavastatin in 421C/C\*1b/\*1b subjects (closed triangles,  $n = 11$ ), 421C/C\*1b/\*15 subjects (open circles,  $n = 8$ ), and 421C/A\*15/\*15 subjects (closed circles,  $n = 3$ ).

*SLCO1B1*\*1b allele showed more enhanced transport activity than the \*1a allele.<sup>17,21</sup>

Systematic mutation analysis of the *ABCG2* gene has been performed in various ethnic populations and more than 40 single nucleotide polymorphisms have been identified.<sup>22–25</sup> The two most frequent nonsynonymous mutations identified in humans are 34G>A (12Val>Met in exon 2) and 421C>A (141Gln>Lys in exon 5). After intravenous administration, plasma levels of diflomotecan were significantly higher in patients with the 421C/A than the 421C/C genotype.<sup>26</sup> These results were supported by *in vitro* experiments showing that BCRP expression of the 421C>A variant was reduced compared with the wild-type,<sup>22,27,28</sup> suggesting that carriers of the 421C>A variant may have decreased clearance (increased plasma levels) and/or increased bioavailability.

In view of the pharmacokinetics, at least two genes (*i.e.*, *SLCO1B1* and *ABCG2*) are of interest as candidates that may lead to large interindividual variability in the pharmacokinetics and clinical outcome of pitavastatin therapy. Recently, Chung *et al.*<sup>18</sup> evaluated the contribution of *SLCO1B1* haplotypes to pitavastatin pharmacokinetics and demonstrated that subjects with the \*15 allele showed significantly higher dose-normalized pitavastatin plasma levels. Although these observations are similar trends to pravastatin, no homozygotes for the \*15 allele participated in their study. Very recently, Zhang *et al.*<sup>29</sup> studied the role of *ABCG2* 421C>A variant in rosuvastatin pharmacokinetics in 14 healthy volunteers and indicated that the AUC of rosuvastatin was lower in the 421C/C group than in the (421C/A and 421A/A) group. Although all statins share a common action mechanism, they differ in terms of their chemical structures, pharmacokinetics, and pharmacodynamics.<sup>30</sup>

With this background in mind, we designed this study to confirm the role of *SLCO1B1* and *ABCG2* polymorphisms in the pharmacokinetics of pitavastatin in healthy volunteers. In this study, we selected volunteers from our panels based on their genotypes of *SLCO1B1* (\*1b and \*15) and *ABCG2* (421C>A). In addition, we investigated the importance of intestinal BCRP in the pharmacokinetics of pitavastatin using Bcrp1 (–/–) mice.

## RESULTS

No clinically undesirable signs and symptoms possibly attributed to the administration of pitavastatin were recognizable throughout the study. All subjects completed the study successfully according to the protocol.

### Pitavastatin pharmacokinetics in relation to *SLCO1B1* and *ABCG2* genotypic status

After oral administration, the mean plasma concentrations of pitavastatin were significantly higher ( $P < 0.01$ ) in group 3 subjects ( $n = 3$ , homozygotes for the *SLCO1B1*\*15 allele, 421C/C\*15/\*15 ( $n = 2$ ) and 421C/A\*15/\*15 ( $n = 1$ )) compared with group 1 subjects ( $n = 11$ , homozygotes for the *SLCO1B1*\*1b allele, 421C/C\*1b/\*1b), and group 2 subjects, heterozygotes for the *SLCO1B1*\*15 allele ( $n = 8$ , 421C/C\*1b/\*15), had values between those in group 1 (*i.e.*, \*1b/\*1b) and group 3 (\*15/\*15) subjects at all observation points (Figure 1). The mean ( $\pm$ SD) AUC<sub>0–24</sub> of pitavastatin in groups 1 (\*1b/\*1b), 2 (421C/C\*1b/\*15), 3 (\*15/\*15), and 6 (421C/A\*1b/\*15) was  $81.1 \pm 18.1$ ,  $144 \pm 32$ ,  $250 \pm 57$ , and  $121 \pm 25$  ng h/ml, respectively. The mean apparent oral clearance (CL<sub>t</sub>) of pitavastatin in groups 1 (\*1b/\*1b), 2 (421C/C\*1b/\*15), 3 (\*15/\*15), and 6 (421C/A\*1b/\*15) was  $0.43 \pm 0.13$ ,  $0.24 \pm 0.04$ ,  $0.15 \pm 0.03$ , and  $0.29 \pm 0.07$  l/h/kg, respectively. The group 3 (\*15/\*15) subjects had the highest AUC value and the lowest CL<sub>t</sub> value among all study volunteers. A similar trend was observed in peak concentration ( $C_{max}$ ) values, but not in elimination rate constant ( $K_e$ ) values. Although the difference did not reach the level of significance, volume of distribution/bioavailability ( $V_d/F$ ) values tended to be lower in subjects with the \*15 allele; the mean  $V_d/F$  in group 3 (\*15/\*15) was 30% of that in group 1 (\*1b/\*1b). In contrast to pitavastatin, no significant intergenotypic differences were observed in any mean pharmacokinetic parameters of pitavastatin lactone in this experiment (Table 1 and Figure 1).

The mean plasma concentration–time curves of pitavastatin and pitavastatin lactone in relation to *ABCG2* genotypic status are shown in Figure 2. The pharmacokinetic parameters are also summarized in Table 1. There were no significant differences in any of the pharmacokinetic

**Table 1 Pharmacokinetic parameters of pitavastatin and its lactone form in each genotyping group**

Genotype		n	Pitavastatin					Pitavastatin lactone		
<i>SLCO1B1</i>	<i>ABCG2</i>		AUC <sub>0-24</sub> (ng h/ml)	CL <sub>t</sub> (l/h/kg)	C <sub>max</sub> (ng/ml)	K <sub>e</sub> (per hour)	V <sub>d</sub> /F (l/kg)	AUC <sub>0-24</sub> (ng h/ml)	C <sub>max</sub> (ng/ml)	K <sub>e</sub> (per hour)
*1b/*1b	421C/C	11	81.1 ± 18.1	0.43 ± 0.13	31.2 ± 11.4	0.06 ± 0.03	0.58 ± 0.27	154 ± 27	20.4 ± 4.4	0.07 ± 0.01
*1b/*15	421C/C	8	144 ± 32 <sup>a</sup>	0.24 ± 0.04 <sup>a</sup>	70.7 ± 18.1 <sup>a</sup>	0.06 ± 0.02	0.27 ± 0.09	169 ± 38	22.3 ± 5.4	0.08 ± 0.02
*15/*15	421C/C 421C/A	3	250 ± 57 <sup>a,b</sup>	0.15 ± 0.03 <sup>a</sup>	129 ± 24 <sup>a</sup>	0.06 ± 0.01	0.16 ± 0.07	153 ± 31	27.2 ± 8.8	0.07 ± 0.01
*1b/*1b	421C/A	7	96.7 ± 35.4	0.37 ± 0.13	41.7 ± 12.4	0.06 ± 0.03	0.46 ± 0.25	145 ± 38	18.9 ± 3.1	0.06 ± 0.02
*1b/*1b	421A/A	3	78.2 ± 8.2	0.42 ± 0.01	42.1 ± 6.3	0.05 ± 0.02	0.48 ± 0.21	140 ± 47	22.1 ± 4.9	0.06 ± 0.01
*1b/*15	421C/A	6	121 ± 25	0.29 ± 0.07	57.7 ± 7.6	0.05 ± 0.01	0.26 ± 0.05	125 ± 18	18.8 ± 2.6	0.07 ± 0.01

AUC<sub>0-24</sub>, area under plasma concentration-time curve from 0 to 24 h; CL<sub>t</sub>, total clearance; C<sub>max</sub>, peak concentration; V<sub>d</sub>/F, volume of distribution/bioavailability. Data are presented as the mean ± SD. <sup>a</sup>Significantly different from values in *SLCO1B1*\*1b/\*1b421C/C subjects as determined by analysis of variance with Fisher's least significant difference test ( $P < 0.01$ ). <sup>b</sup>Significantly different from values in *SLCO1B1*\*1b/\*15421C/C subjects as determined by analysis of variance with Fisher's least significant difference test ( $P < 0.01$ ).

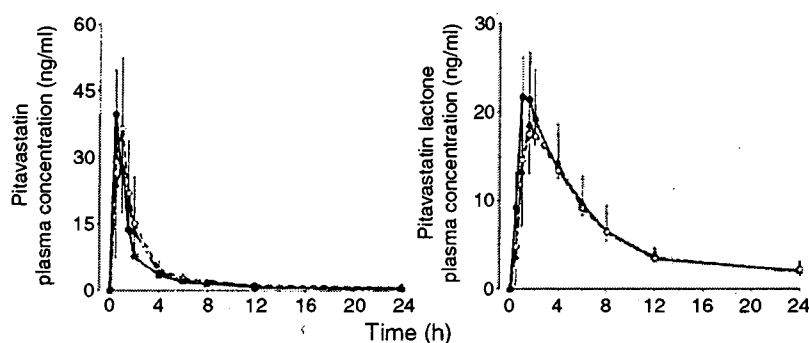


**Figure 2** Effect of *ABCG2* genotype on pharmacokinetics of pitavastatin. Plasma concentration-time profiles of pitavastatin and pitavastatin lactone after oral administration of 2 mg pitavastatin in 421C/C\*1b/\*1b subjects (closed triangles,  $n = 11$ ), 421C/A\*1b/\*1b subjects (open circles,  $n = 7$ ), and 421A/A\*1b/\*1b subjects (closed circles,  $n = 3$ ).

parameters for either pitavastatin or pitavastatin lactone among the three *SLCO1B1* matched (*i.e.*, homozygotes for the \*1b allele) *ABCG2* groups: group 1 ( $n = 11$ , 421C/C\*1b/\*1b), group 4 ( $n = 7$ , 421C/A\*1b/\*1b), and group 5 ( $n = 3$ , 421A/A\*1b/\*1b). The mean AUC<sub>0-24</sub> of pitavastatin in groups 1 (*i.e.*, 421C/C), 4 (421C/A\*1b/\*1b), 5 (421A/A), and 6 (421C/A\*1b/\*15) was  $81.1 \pm 18.1$ ,  $96.7 \pm 35.4$ ,  $78.2 \pm 8.2$ , and  $121 \pm 25$  ng h/ml, respectively.

#### Role of BCRP in the intestinal absorption of pitavastatin in mice *in vivo*

To investigate the involvement of Bcrp1 in the intestinal absorption of pitavastatin, we evaluated its pharmacokinetics using control and Bcrp1 (-/-) mice. The mean AUC up to 4 h after administration was  $213 \pm 13$  and  $221 \pm 17$  ng h/ml (mean ± SE,  $n = 4$ ) in control and Bcrp1 (-/-) mice, respectively ( $P > 0.05$ ). The time profiles of the plasma concentration of pitavastatin did not show any significant difference between control and Bcrp1 (-/-) mice (**Figure 3**).

#### DISCUSSION

The primary objective of this study was to evaluate whether the polymorphism of two drug transporter genes contribute to large interindividual variability in the pharmacokinetics of

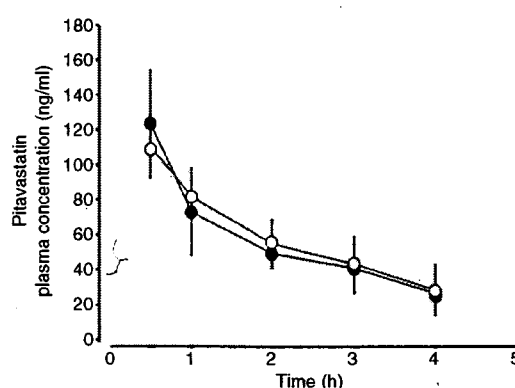


**Figure 3** Time profiles of plasma concentration of pitavastatin after its oral administration (10 mg/kg) to control and Bcrp1 (-/-) mice. Closed and open circles represent the time profile of plasma concentration of pitavastatin in control and Bcrp1 (-/-) mice, respectively.

pitavastatin, a dual substrate of OATP1B1 and BCRP. The important findings were that (1) significant differences in AUC<sub>0-24</sub> and C<sub>max</sub> of pitavastatin, but not in those of the lactone form, were observed among subjects with different *SLCO1B1* genotypes; and (2) in contrast to *SLCO1B1*, no significant differences in any pharmacokinetic parameters

were observed among genotyping groups of *ABCG2*. To ensure the quality of the study, we selected *SLCO1B1* and *ABCG2* genotyping-matched volunteers from our panels. However, unfortunately, as the frequency of the *SLCO1B1*\*15/\*15 is low in Japanese populations,<sup>15</sup> we recruited one miss-matched 421C/A subject in group 3 (*i.e.*, \*15/\*15), which could have consequences for the interpretation of the results.

In this study, the mean  $AUC_{0-24}$  and  $C_{max}$  values in homozygotes for the *SLCO1B1*\*15 allele were 3.1- and 4.1-fold higher, respectively, than those in *SLCO1B1*\*1b/\*1b subjects, and heterozygotes had values between the two homozygous groups. These findings were consistent with a recent study conducted by Chung *et al.*<sup>18</sup> Although no homozygotes for the \*15 allele were included in their study, they found dose-normalized AUC and  $C_{max}$  of pitavastatin to be 1.4- and 1.8-fold higher, respectively, in subjects heterozygous for the \*15 allele versus subjects without this allele. Several transporters are known to be involved in the hepatic uptake of clinically important drugs in humans. Among them, a recent *in vitro* study indicated that the uptake clearance of pitavastatin in human hepatocytes could be almost completely accounted for by OATP1B1 and OATP1B3 (OATP8), but approximately 90% of the total hepatic clearance could be accounted for by OATP1B1.<sup>6</sup> Thus, similar to pravastatin, OATP1B1 is suggested to play an important role in the hepatic uptake of pitavastatin in humans.

The 174Val>Ala variant has been consistently associated with reduced transport activity of OATP1B1 both *in vitro*<sup>14,31</sup> and *in vivo*.<sup>15-18</sup> As selective distribution to the liver may also be the first step for the pharmacological action of pitavastatin, subjects with this variant (*i.e.*, \*5, \*15, and \*17 alleles) are expected to exhibit a reduced cholesterol-lowering effect owing to the lower pitavastatin concentration in hepatocytes, despite high plasma concentrations and AUC of pitavastatin. To date, some groups have reported the implication of the *SLCO1B1* polymorphism in the lipid-lowering efficacy of statins under multiple-dose conditions<sup>32</sup> and chronic treatment.<sup>33-35</sup> Igel *et al.*<sup>32</sup> conducted a healthy volunteer study ( $n=16$ ) and demonstrated no significant difference in the lipid-lowering efficacy of pravastatin between the variant allele (\*15 and \*17 alleles) and control groups after treatment with 40 mg pravastatin daily for 3 weeks, despite considerably higher plasma pravastatin concentration in the variant group. Similarly, in a study of 33 patients with hypercholesterolemia treated with pravastatin (mean dose of 9.4 mg/day), the genotype-dependent difference in the lipid-lowering effect in the initial phase of treatment (8 weeks) disappeared after 1 year of treatment.<sup>33</sup> In addition to experimental designs, such as the male/female ratio<sup>36</sup> and racial background, numerous genetic factors may have an impact on the response to statins.<sup>32,37</sup> Furthermore, the 174Val>Ala variant is associated with reduced transport activity, but does not lead to loss of activity,<sup>14,31</sup> making it conceivable that there is no significant impact of the

genotype on the clinical efficacy of statins during long-term treatment; however, a high plasma concentration, on the other hand, is known as a risk factor for the myotoxic effects of statins.<sup>38</sup> The effect of the polymorphism of the *SLCO1B1* gene on the clinical efficacy and adverse events of pitavastatin will be the subject of further investigation.

In this study, the  $AUC_{0-24}$  of the lactone form was comparable with that of the acid form, and the pharmacokinetics of lactone was not affected by the *SLCO1B1* polymorphism. The profile of the hepatic uptake of lactone has not yet been elucidated; however, our study indicated that OATP1B1 can be ruled out as a candidate transporter in humans. As the lactone form can be reversibly converted to the acid form in the body, it can be asked whether a comparably high serum concentration of lactone contributes to the clinical efficacy of pitavastatin. In the acid/lactone interconversion of pitavastatin, the following pathways have been proposed: the first step is the glucuronidation of pitavastatin to form UM-2 as an intermediate to the lactone form by uridine 5'-diphosphate glucuronosyl transferases (UGT1A1, 1A3, and 2B7). The glucuronic acid moiety is subsequently converted nonenzymatically to its lactone form. After conversion, some of the resulting lactone form changes to the acid form by hydrolysis. Cytochrome p450 3A4-mediated metabolism of the lactone form was also observed in human hepatic microsomes.<sup>3,4</sup> Furthermore, in addition to the liver, lactone may form in extrahepatic tissues such as the kidney and intestine.<sup>4</sup> Although the metabolism of pitavastatin is complex, lactonization is the major metabolic pathway in humans.<sup>4</sup> These findings suggest that a certain amount of pitavastatin acid produced from the lactone form by hepatic interconversion has a clinical impact on the lipid-lowering effect. Further study with regard to the *SLCO1B1* polymorphism, in which the pitavastatin lactone form is used as a test drug, is required.

In addition to  $AUC_{0-24}$ , the mean  $C_{max}$  was higher in subjects with the \*15 allele than in subjects without this allele. To discuss this point, we estimated the pharmacokinetic data using WinNonlin. Although the difference did not reach the level of significance,  $V_d/F$  values tended to be lower in subjects with the \*15 allele (Table 1). The  $V_d$  of pitavastatin in the liver ( $V_{dliver}$ ) can be estimated by the following equation:  $K_{Pliver} \times V_{dliver}$ , where  $K_{Pliver}$  is the  $C_{Pliver}/C_{Pplasma}$  ratio (approximately 23.0 in rats),<sup>9</sup> and  $V_{dliver}$  is the liver volume (approximately 78.4 ml/kg).<sup>39</sup> Estimated  $V_{dliver}$  (1.8 l/kg) and  $V_d/F$  (1.0 l/kg)<sup>9</sup> are comparable, suggesting that the liver is the major organ for the distribution of pitavastatin in rats. In addition, total clearance of pitavastatin (0.15–0.43 l/h/kg in this study) is relatively lower than that of other statins in humans (800–1000 l/h for simvastatin,<sup>40</sup> 0.8–2.7 l/h/kg for pravastatin,<sup>15</sup> 80–200 l/h for rosuvastatin,<sup>41</sup> and 150–1200 l/h for atorvastatin<sup>42</sup>). Taking these *in vivo* findings into consideration, a decreased  $V_d$  of pitavastatin owing to low transport activity is one of the possible reasons for high  $C_{max}$  values in subjects with the \*15 allele. Nevertheless, changes in  $F$  cannot be denied in such subjects because there is no



intravenous data for pitavastatin to determine absolute value of bioavailability.

In this study, no change in  $K_e$  values was observed. Although a firm conclusion cannot be reached regarding possible changes in  $V_d$  versus  $F$  (again, because of no intravenous data), *OATP1B1\*15* allele may be associated with decreased  $CL_t$  and  $V_d$  values simultaneously, which may cancel out the change in  $K_e$  values.

It was somewhat unexpected that there were no significant differences in any pharmacokinetic parameters among *ABCG2* (421C>A) genotypic groups because some *in vivo* studies demonstrated that the 421C>A allele was associated with changes in the pharmacokinetics of certain clinically important substrate drugs, such as diflomotecan<sup>26</sup> and topotecan.<sup>45</sup> In addition, Zhang *et al.*<sup>29</sup> recently studied rosuvastatin pharmacokinetics in relation to the *ABCG2* 421C>A polymorphism in 14 healthy volunteers. Although they used an insufficient number of subjects, they demonstrated that the AUC of rosuvastatin was lower in subjects with the 421C/C genotype than in subjects with 421A variant(s). Available data indicate that the 421C>A variant was associated with remarkably decreased BCRP expression compared with wild-type cells and human placental samples,<sup>22,27</sup> which may lead to the following changes based on its localization; increased absorption at the intestinal epithelium, and/or decreased biliary excretion of substrates, thereby resulting in elevated plasma concentrations in subjects with 421A variant(s). Although both pitavastatin and rosuvastatin seem to be good substrates for BCRP,<sup>9,44</sup> our present findings were clearly in contrast to the findings reported by Zhang *et al.*<sup>29</sup> This discrepancy may be explained as follows: a recent *in vitro* experiment using double-transfected Madin-Darby canine kidney (MDCK) II monolayers expressing OATP1B1 and human canalicular efflux transporters indicated that the significant transport of pitavastatin was observed in OATP1B1/MDR1 and OATP1B1/MRP2 as well as OATP1B1/BCRP double transfectants.<sup>9</sup> These results suggest that multiple organic anion transporters across the canalicular membrane in the liver are involved in the biliary excretion of pitavastatin.

Hirano *et al.*<sup>9</sup> have previously shown that the biliary excretion of pitavastatin in *Bcrp1* (−/−) mice was drastically reduced compared with that in control mice after constant infusion, although the steady-state plasma concentration in *Bcrp1* (−/−) mice is not different from that in control mice owing to the extensive metabolism of pitavastatin in mice. As BCRP is also expressed on the brush-border membrane of enterocytes, reduced function because of modulation of the expression level or recognition/affinity capability may lead to the increasing intestinal absorption of substrate drugs; therefore, we compared the pharmacokinetics of pitavastatin after oral administration in *Bcrp1* (−/−) and control mice. Similar to the constant infusion, the time profiles of the plasma concentration of pitavastatin were not different between *Bcrp1* (−/−) and control mice (Figure 3). These results suggest that, in contrast to the biliary excretion, *Bcrp1*

is not important as a determinant of intestinal absorption. In our animal study, the dose of pitavastatin was considerably higher and also the plasma concentrations appeared to be somewhat higher in mice than those observed in our subjects. In addition to these experimental designs, the metabolic profile of pitavastatin is reported to be different between mice and men;<sup>9</sup> however, our present findings suggest that the contribution of BCRP to the pharmacokinetics of pitavastatin is not significant as our expectations in humans.

Although all statins share a common action mechanism, they differ in terms of their chemical structures, pharmacokinetics, and pharmacodynamics. In particular, transporters involved in biliary excretion are different among statins; for example, *ABCC2* (MRP2) is reported to be responsible for pravastatin both *in vitro* and *in vivo*.<sup>9,45,46</sup> In addition to efflux, a recent study indicated that multiple transporters are involved in the hepatic uptake of statins.<sup>47</sup> These differences make the understanding of the transport mechanism of statins difficult. Differences in the pharmacokinetic profiles between acid and lactone forms of pitavastatin observed in this study can be partially attributed to the contribution of multiple transporters.<sup>48</sup> However, hepatic uptake of pravastatin and pitavastatin, and probably rosuvastatin,<sup>41</sup> by OATP1B1 seems to be the major determinant of their overall pharmacokinetic profiles (*i.e.*, elimination and tissue distribution) in humans. Indeed, numerous OATP1B1-mediated drug–drug interactions have been reported to date, suggesting that transporter-mediated hepatic uptake is the main determinant of plasma clearance, even for drugs undergoing extensive metabolism.<sup>49</sup>

## METHODS

**Subjects and genotyping of *SLCO1B1* and *ABCG2*.** After approval by the Ethics Review Board of Kyushu University and Kyushu Clinical Pharmacology Research Clinic, 38 healthy male volunteers (age, 20–32 years; weight, 52.4–72.4 kg) gave written informed consent to participate in the study. None had taken any drugs for at least 1 week before the study. Each subject was physically normal and had no antecedent history of significant medical illness or hypersensitivity to any drugs, and each had a body mass index between 17.6 and 26.4 kg/m<sup>2</sup>. Their health status was judged to be normal on the basis of a physical examination with screening of blood chemistry, a complete blood count and urinalysis, and an electrocardiogram just before the study.

The genotyping methods of *SLCO1B1* and *ABCG2* have been described previously.<sup>15,22</sup> Single-strand conformation polymorphism and polymerase chain reaction–restriction fragment length polymorphism methods were used for genotyping. In this study, \*1b and \*15 alleles and 421C>A variant were identified for *SLCO1B1* and *ABCG2* genes, respectively, and all subjects were divided into the following groups: 421C/C\*1b/\*1b (group 1,  $n = 11$ ), 421C/C\*1b/\*15 (group 2,  $n = 8$ ), 421C/C\*15/\*15 ( $n = 2$ ) and 421C/A\*15/\*15 ( $n = 1$ ) (group 3), 421C/A\*1b/\*1b (group 4,  $n = 7$ ), 421A/A\*1b/\*1b (group 5,  $n = 3$ ), and 421C/A\*1b/\*15 (group 6,  $n = 6$ ).

**Study protocol.** The participants came to the clinic after an overnight fast. They were required to abstain from alcohol for 2 days before drug administration and during the period of hospitalization and were served standard meals on the study day. Each volunteer received a single oral dose of 2 mg of pitavastatin (Livalo, Kowa,

Nagoya, Japan) with 150 ml of water. Venous blood samples (7 ml each) to determine pitavastatin and pitavastatin lactone concentrations were obtained just before and 0.5, 1, 1.5, 2, 4, 6, 8, 12, and 24 h after dosing. Plasma samples were immediately separated after centrifugation and stored at  $-70^{\circ}\text{C}$  until analyzed.

**Quantification of pitavastatin and pitavastatin lactone in plasma.** The concentrations of pitavastatin and its lactone in plasma were measured by high-performance liquid chromatography (HPLC) according to the methods of Kojima *et al.*<sup>50</sup> with a minor modification. The plasma sample (1.0 ml) was mixed with 0.2 ml internal standard (I-1938, 125 ng/ml; supplied by Nissan Chemical Industries (Saitama, Japan)), 0.2 ml water, 10  $\mu\text{l}$  acetonitrile, and 0.5 ml 1.0 M potassium dihydrogenphosphate in a colored tube. The sample mixture was extracted with 8 ml of methyl *tert*-butyl ether by shaking for 10 min on a horizontal shaker at 200 r.p.m. and by centrifuging for 10 min at approximately  $1,720 \times g$  (at  $4^{\circ}\text{C}$ ). The organic layer was transferred to another colored tube and subsequently diazomethane-diethyl ether solution (0.5 ml) was added. The reaction mixture was kept at room temperature for 30 min. To degrade excessive diazomethane, 1.0 M potassium dihydrogenphosphate (2 ml) was added to the mixture. After centrifuging for 10 min at  $1,720 \times g$ , the organic layer was evaporated to dryness under a gentle stream of nitrogen at  $40^{\circ}\text{C}$ . The residue was reconstituted in 150  $\mu\text{l}$  of mobile phase for pre-separation and an aliquot of 80  $\mu\text{l}$  was injected into the HPLC system. Column-switching HPLC (using a six-port switching valve) was performed with two Cosmosil-C18-MS-II columns ( $150 \times 4.6$  mm internal diameter; Nacalai Tesque, Kyoto, Japan) for pre-separation and analytical separation. Two mobile phases, 0.2 M ammonium acetate buffer (pH 4.0)-acetonitrile (5:5, v/v) for pre-separation and 0.2 M acetic acid-acetonitrile (5:5, v/v) for analytical separation, were maintained at a flow rate of 1.0 ml/min. Detection was carried out at 250 nm with a UV detector. Column temperature was maintained at  $40^{\circ}\text{C}$ . Calibration curves for both analytes ranged from 0.5 to 200 ng/ml. This HPLC method was validated only for the measurement of serum concentrations of pitavastatin and lactone in the human study. The intraday coefficient of variation values were less than 13.0% and intraday accuracies were between  $-14.0$  and 6.0%, within the concentration range of the calibration curves for both analytes. Interday coefficient of variation values were less than 5.0% and interday accuracies were between  $-2.4$  and 4.7%. The limits of quantification for both analytes were set to 0.5 ng/ml.<sup>50</sup>

**In vivo study in mice and quantification of pitavastatin by liquid chromatography/mass spectrometry.** Male FVB control and Bcrp1 ( $-/-$ ) mice weighing approximately 28–33 g were used throughout these experiments. Pitavastatin was orally administered to both mice at a dose of 10 mg/kg. Blood samples were collected from the tail vein at 0.5, 1, 2, 3, and 4 h after oral administration of pitavastatin. The plasma sample (10  $\mu\text{l}$ ) was mixed with 100  $\mu\text{l}$  methanol containing the internal standard (atorvastatin, 80 ng/ml), followed by centrifugation ( $10,000 \times g$ ) at  $4^{\circ}\text{C}$  for 10 min. Atorvastatin was synthesized by Kowa (Tokyo, Japan). The supernatant (80  $\mu\text{l}$ ) was mixed with 50  $\mu\text{l}$  water and subjected to HPLC (Waters 2695; Waters, Milford, MA). Liquid chromatography/mass spectrometry analysis of pitavastatin was performed with an Inertsil ODS-3 column ( $50 \times 2.1$  mm internal diameter, particle size 5  $\mu\text{m}$ ) (GL Sciences, Tokyo, Japan). The mobile phase consisted of methanol-ammonium formate buffer (pH 4.0, 7:3, v/v) and the flow rate was 0.5 ml/min. The mass spectrometry instrument used for this work was a ZQ micro-mass (Waters) equipped with a Z-spray source and operated in the positive-ion electrospray ionization mode. The Z-spray desolvation temperature, capillary voltage, and cone voltage were  $350^{\circ}\text{C}$ , 3400 V and 40 V, respectively. The *m/z* monitored for pitavastatin and atorvastatin was 422.3 and 559.0, respectively. No

chromatographic interference was found for pitavastatin and atorvastatin in extracts from blank plasma. The retention times of pitavastatin and atorvastatin were 1.5 and 1.4 min, respectively. The calibration curves for pitavastatin ranged from 5 to 1000 ng/ml. This liquid chromatography/mass spectrometry method was validated only for the measurement of serum concentration of pitavastatin in the animal study. For pitavastatin, quality control samples covering the whole concentration range showed high intra- and interday accuracy and reproducibility with a coefficient of variation and bias below 10%.

**Pharmacokinetics and statistical analysis.**  $C_{\text{max}}$  was obtained directly from the data.  $\text{AUC}_{0-24}$  was calculated by the linear trapezoidal rule. We calculated the  $\text{CL}_t$  of pitavastatin as follows:  $\text{CL}_t = \text{Dose}/\text{AUC}_{0-24}$ . The  $K_e$  was estimated using least-squares regression analysis from the terminal postdistribution phase of the concentration-time curve. To assess differences in the  $V_d/F$  of pitavastatin in relation to the *SLCO1B1* polymorphism, we also estimated model-dependent parameters (one-compartment open model with first-order elimination and no lag time) using the WinNonlin 5.0.1 program (Pharsight, Mountain View, CA). Statistical differences among the data for each group were determined by analysis of variance, followed by Fisher's least significant difference test.  $P < 0.05$  was considered statistically significant.

#### ACKNOWLEDGMENTS

This study was supported by a Health and Labour Sciences Research Grant from the Ministry of Health, Labour and Welfare for Research on Advanced Medical Technology.

#### CONFLICT OF INTEREST

The authors declared no conflict of interest.

© 2007 American Society for Clinical Pharmacology and Therapeutics

- Aoki, T. *et al.* Pharmacological profile of a novel synthetic inhibitor of 3-hydroxy-3-methylglutaryl-coenzyme A reductase. *Arzneimittelforschung* **47**, 904–909 1997.
- Fujino, H., Yamada, I., Shimada, S., Nagao, T. & Yoneda, M. Metabolic fate of pitavastatin (NK-104), a new inhibitor of 3-hydroxy-3-methyl-glutaryl coenzyme A reductase. Effects on drug-metabolizing systems in rats and humans. *Arzneimittelforschung* **52**, 745–753 2002.
- Fujino, H., Saito, T., Tsunenari, Y., Kojima, J. & Sakaeda, T. Metabolic properties of the acid and lactone forms of HMG-CoA reductase inhibitors. *Xenobiotica* **34**, 961–971 2004.
- Fujino, H., Yamada, I., Shimada, S., Yoneda, M. & Kojima, J. Metabolic fate of pitavastatin, a new inhibitor of HMG-CoA reductase: human UDP-glucuronosyltransferase enzymes involved in lactonization. *Xenobiotica* **33**, 27–41 2003.
- Yamada, I., Fujino, H., Shimada, S. & Kojima, J. Metabolic fate of pitavastatin, a new inhibitor of HMG-CoA reductase: similarities and difference in the metabolism of pitavastatin in monkeys and humans. *Xenobiotica* **33**, 789–803 2003.
- Hirano, M., Maeda, K., Shitara, Y. & Sugiyama, Y. Contribution of OATP2 (OATP1B1) and OATP8 (OATP1B3) to the hepatic uptake of pitavastatin in humans. *J. Pharmacol. Exp. Ther.* **311**, 139–146 2004.
- Hagenbuch, B. & Meier, P.J. The superfamily of organic anion transporting polypeptides. *Biochim. Biophys. Acta* **1609**, 1–18 2003.
- Hsiang, B. *et al.* A novel human hepatic organic anion transporting polypeptide (OATP2). Identification of a liver-specific human organic anion transporting polypeptide and identification of rat and human hydroxymethylglutaryl-CoA reductase inhibitor transporters. *J. Biol. Chem.* **274**, 37161–37168 1999.
- Hirano, M., Maeda, K., Matsushima, S., Nozaki, Y., Kusuhara, H. & Sugiyama, Y. Involvement of BCRP (ABCG2) in the biliary excretion of pitavastatin. *Mol. Pharmacol.* **68**, 800–807 2005.
- Cervenak, J. *et al.* The role of the human ABCG2 multidrug transporter and its variants in cancer therapy and toxicology. *Cancer Lett.* **234**, 62–72 2006.

11. Maliapaard, M. *et al.* Subcellular localization and distribution of the breast cancer resistance protein transporter in normal human tissues. *Cancer Res.* **61**, 3458-3464 2001.
12. Kruijtzter, C.M., Beijnen, J.H. & Schellens, J.H. Improvement of oral drug treatment by temporary inhibition of drug transporters and/or cytochrome P450 in the gastrointestinal tract and liver: an overview. *Oncologist* **7**, 516-530 2002.
13. Taipalensuu, J. *et al.* Correlation of gene expression of ten drug efflux proteins of the ATP-binding cassette transporter family in normal human jejunum and in human intestinal epithelial Caco-2 cell monolayers. *J. Pharmacol. Exp. Ther.* **299**, 164-170 2001.
14. Tirona, R.G., Leake, B.F., Merino, G. & Kim, R.B. Polymorphisms in OATP-C: identification of multiple allelic variants associated with altered transport activity among European- and African-Americans. *J. Biol. Chem.* **276**, 35669-35675 2001.
15. Nishizato, Y. *et al.* Polymorphisms of OATP-C (SLC21A6) and OAT3 (SLC22A8) genes: consequences for pravastatin pharmacokinetics. *Clin. Pharmacol. Ther.* **73**, 554-565 2003.
16. Niemi, M. *et al.* High plasma pravastatin concentrations are associated with single nucleotide polymorphisms and haplotypes of organic anion transporting polypeptide-C (OATP-C SLCO1B1). *Pharmacogenetics* **14**, 429-440 2004.
17. Mwinyi, J., Johne, A., Bauer, S., Roots, I. & Gerloff, T. Evidence for inverse effects of OATP-C (SLC21A6) 5 and 1b haplotypes on pravastatin kinetics. *Clin. Pharmacol. Ther.* **75**, 415-421 2004.
18. Chung, J.Y. *et al.* Effect of OATP1B1 (SLCO1B1) variant alleles on the pharmacokinetics of pitavastatin in healthy volunteers. *Clin. Pharmacol. Ther.* **78**, 342-350 2005.
19. Niemi, M., Kivisto, K.T., Hofmann, U., Schwab, M., Eichelbaum, M. & Fromm, M.F. Fexofenadine pharmacokinetics are associated with a polymorphism of the SLCO1B1 gene (encoding OATP1B1). *Br. J. Clin. Pharmacol.* **59**, 602-604 2005.
20. Niemi, M. *et al.* Polymorphic organic anion transporting polypeptide 1B1 is a major determinant of repaglinide pharmacokinetics. *Clin. Pharmacol. Ther.* **77**, 468-478 2005.
21. Maeda, K. *et al.* Effects of organic anion transporting polypeptide 1B1 haplotype on pharmacokinetics of pravastatin, valsartan, and temocapril. *Clin. Pharmacol. Ther.* **79**, 427-439 2006.
22. Kobayashi, D. *et al.* Functional assessment of ABCG2 (BCRP) gene polymorphisms to protein expression in human placenta. *Drug Metab. Dispos.* **33**, 94-101 2005.
23. Iida, A. *et al.* Catalog of 605 single-nucleotide polymorphisms (SNPs) among 13 genes encoding human ATP-binding cassette transporters: ABCA4, ABCA7, ABCA8, ABCD1, ABCD3, ABCD4, ABCE1, ABCF1, ABCG1, ABCG2, ABCG4, ABCG5, and ABCG8. *J. Hum. Genet.* **47**, 285-310 2002.
24. Zamber, C.P. *et al.* Natural allelic variants of breast cancer resistance protein (BCRP) and their relationship to BCRP expression in human intestine. *Pharmacogenetics* **13**, 19-28 2003.
25. Backstrom, G. *et al.* Genetic variation in the ATP-binding cassette transporter gene ABCG2 (BCRP) in a Swedish population. *Eur. J. Pharm. Sci.* **18**, 359-364 2003.
26. Sparreboom, A. *et al.* Diflomotecan pharmacokinetics in relation to ABCG2 421C>A genotype. *Clin. Pharmacol. Ther.* **76**, 38-44 2004.
27. Kondo, C. *et al.* Functional analysis of SNPs variants of BCRP/ABCG2. *Pharm. Res.* **21**, 1895-1903 2004.
28. Imai, Y. *et al.* C421A polymorphism in the human breast cancer resistance protein gene is associated with low expression of Q141K protein and low-level drug resistance. *Mol. Cancer Ther.* **1**, 611-616 2002.
29. Zhang, W. *et al.* Role of BCRP 421C>A polymorphism on rosuvastatin pharmacokinetics in healthy Chinese males. *Clin. Chim. Acta* **373**, 99-103 2006.
30. Schachter, M. Chemical, pharmacokinetic and pharmacodynamic properties of statins: an update. *Fundam. Clin. Pharmacol.* **19**, 117-125 2005.
31. Kameyama, Y., Yamashita, K., Kobayashi, K., Hosokawa, M. & Chiba, K. Functional characterization of SLCO1B1 (OATP-C) variants, SLCO1B1\*5, SLCO1B1\*15 and SLCO1B1\*15+C1007G, by using transient expression systems of HeLa and HEK293 cells. *Pharmacogenet. Genomics* **15**, 513-522 2005.
32. Igel, M. *et al.* Impact of the SLCO1B1 polymorphism on the pharmacokinetics and lipid-lowering efficacy of multiple-dose pravastatin. *Clin. Pharmacol. Ther.* **79**, 419-426 2006.
33. Takane, H. *et al.* Pharmacogenetic determinants of variability in lipid-lowering response to pravastatin therapy. *J. Hum. Genet.* **51**, 822-826 2006.
34. Tachibana-Iimori, R. *et al.* Effect of genetic polymorphism of OATP-C (SLCO1B1) on lipid-lowering response to HMG-CoA reductase inhibitors. *Drug Metab. Pharmacokinet.* **19**, 375-380 2004.
35. Thompson, J.F. *et al.* An association study of 43 SNPs in 16 candidate genes with atorvastatin response. *Pharmacogenomics J.* **5**, 352-358 2005.
36. Niemi, M., Pasanen, M.K. & Neuvonen, P.J. SLCO1B1 polymorphism and sex affect the pharmacokinetics of pravastatin but not fluvastatin. *Clin. Pharmacol. Ther.* **80**, 356-366 2006.
37. Chasman, D.I., Posada, D., Subrahmanyam, L., Cook, N.R., Stanton, V.P. Jr. & Ridker, P.M. Pharmacogenetic study of statin therapy and cholesterol reduction. *JAMA* **291**, 2821-2827 2004.
38. Thompson, P.D., Clarkson, P. & Karas, R.H. Statin-associated myopathy. *JAMA* **289**, 1681-1690 2003.
39. Davies, B. & Morris, T. Physiological parameters in laboratory animals and humans. *Pharm. Res.* **10**, 1093-1095 1993.
40. Pasanen, M.K., Neuvonen, M., Neuvonen, P.J. & Niemi, M. SLCO1B1 polymorphism markedly affects the pharmacokinetics of simvastatin acid. *Pharmacogenet. Genomics* **16**, 873-879 2006.
41. Lee, E. *et al.* Rosuvastatin pharmacokinetics and pharmacogenetics in white and Asian subjects residing in the same environment. *Clin. Pharmacol. Ther.* **78**, 330-341 2005.
42. Hermann, M. *et al.* Exposure of atorvastatin is unchanged but lactone and acid metabolites are increased several-fold in patients with atorvastatin-induced myopathy. *Clin. Pharmacol. Ther.* **79**, 532-539 2006.
43. Sparreboom, A. *et al.* Effect of ABCG2 genotype on the oral bioavailability of topotecan. *Cancer Biol. Ther.* **4**, 650-658 2005.
44. Huang, L., Wang, Y. & Grimm, S. ATP-dependent transport of rosuvastatin in membrane vesicles expressing breast cancer resistance protein. *Drug Metab. Dispos.* **34**, 738-742 2006.
45. Kivisto, K.T. *et al.* Disposition of oral and intravenous pravastatin in MRP2-deficient TR-rats. *Drug Metab. Dispos.* **33**, 1593-1596 2005.
46. Niemi, M. *et al.* Association of genetic polymorphism in ABCG2 with hepatic multidrug resistance-associated protein 2 expression and pravastatin pharmacokinetics. *Pharmacogenet. Genomics* **16**, 801-808 2006.
47. Ho, R.H. *et al.* Drug and bile acid transporters in rosuvastatin hepatic uptake: function, expression, and pharmacogenetics. *Gastroenterology* **130**, 1793-1806 2006.
48. Fujino, H., Saito, T., Ogawa, S. & Kojima, J. Transporter-mediated influx and efflux mechanisms of pitavastatin, a new inhibitor of HMG-CoA reductase. *J. Pharm. Pharmacol.* **57**, 1305-1311 2005.
49. Shitara, Y. & Sugiyama, Y. Pharmacokinetic and pharmacodynamic alterations of 3-hydroxy-3-methylglutaryl coenzyme A (HMG-CoA) reductase inhibitors: drug-drug interactions and interindividual differences in transporter and metabolic enzyme functions. *Pharmacol. Ther.* **112**, 71-105 2006.
50. Kojima, J., Fujino, H., Yosimura, M., Morikawa, H. & Kimata, H. Simultaneous determination of NK-104 and its lactone in biological samples by column-switching high-performance liquid chromatography with ultraviolet detection. *J. Chromatogr. B. Biomed. Sci. Appl.* **724**, 173-180 1999.

# 大規模 SNP タイピングによる 多因子疾患遺伝子の探索

西田奈央, 徳永勝士

ヒトゲノム計画をはじめとする遺伝情報解析の成果としてデータベースに蓄積された600万種を超える一塩基多型 (SNP) のうち, 約50万種のSNPを同時にタイピングすることのできる手法が近年になって実用化された。われわれは, 500K Human Mapping Array Set (Affymetrix社) によるSNPタイピングを効率的に行うためのシステムを構築し, 大規模なケース・コントロール関連分析を行っている。一例として, 睡眠障害の1つであるナルコレプシーの疾患感受性遺伝子の探索研究を紹介する。

## はじめに

現在, ヒトのさまざまな多因子疾患に関わる遺伝子を探索する戦略として最も注目を浴びているのが, 本稿で紹介するゲノムワイド関連分析法である。例を挙げると, 米国NIH (国立衛生研究所) はGWAS (genomewide association study) 計画を提案し, いくつかのcommon diseasesについて大規模な研究チームを公募した。また, 大規模な疫学研究として知られるFramingham Heart Study (フラミンガム研究) で収集された試料のうち9,000検体について, 本稿で紹介する技術を用いて解析することにより, 心, 肺, 血液, 睡眠疾患に関与する遺伝子変異を探索する計画

### [キーワード&略語]

一塩基多型 (SNP), SNPタイピング, ケース・コントロール関連分析, 疾患感受性遺伝子, ナルコレプシー

GWAS: genomewide association study

LD: linkage disequilibrium (連鎖不平衡)

SNP: single nucleotide polymorphism

(一塩基多型)

も発表された。

このような動向の背景には, 多因子疾患感受性遺伝子を探索する統計遺伝学的手法の選択がある。大別して連鎖分析 (linkage analysis) と関連分析 (association analysis) があり, 従来のゲノムワイド探索のほとんどは連鎖分析法が用いられてきた。多数の成功例があるものの, 連鎖分析のみで疾患感受性遺伝子のほとんどを同定するのは困難であると考えられるようになり, また後述する大規模なSNP解析技術の進展も相まって, ゲノムワイド関連分析が大きく取り上げられることとなった。そもそも連鎖分析は患者家族を対象として文字通り疾患遺伝子と多型マーカーの連鎖を検出する手法であり, ゲノム全域に分布する1万から数万種のSNPを用いればよい。一方, 関連分析の代表であるケース・コントロール関連分析法<sup>\*1</sup>は, 非血縁の患者集団と健常者集団を対象として疾患遺伝子と多型マーカーの連鎖不平衡 (LD) を検出する手法であり, ゲノム全域に分布する数十万種以上のSNPを解析することが必要となる<sup>1)</sup> (統計遺伝学手法の原理ならびに集団遺伝学的基础については別書に解説した<sup>2)</sup>。

Search for susceptibility genes to multifactorial diseases by large-scale SNP typing

Nao Nishida/Katsushi Tokunaga: Department of Human Genetics, Graduate School of Medicine, University of Tokyo (東京大学大学院医学系研究科人類遺伝学分野)

ヒトゲノム上には、マイナーアレル頻度が10%以上のSNPsが500万種、マイナーアレル頻度が1%以上のSNPsとなると1,100万種も存在すると試算されており<sup>3)</sup>、これらのSNPsを大規模にかつ正確にタイピングのできる手法の確立が求められてきた。

SNPタイピング法として最もよく知られている方法は、個々の多型部位を含むゲノム断片を特異的にPCR増幅した後にアレルを識別する方法である<sup>4)~7)</sup>。これらの方法では、1,000種程度のSNPのタイピングであれば、PCRプライマーはじめ各種試薬にかかるコストを考えて実用可能であるといえるが、数千、数万種を超える数のSNPをタイピングすることは困難である。一方、近年になって多型部位特異的なPCRを行わずに大規模なSNPタイピングを行う方法が実用化された<sup>8) 9)</sup>。その一つであるAffymetrix社によって確立された方法では、まず制限酵素反応でゲノムDNAの断片化を行い、続いてそれら断片の両端にアダプター配列を付加し、まとめて増幅した後にマイクロアレイを用いたアレル特異的なハイブリダイゼーションを行う<sup>8)</sup>。現在では、この手法を用いて50万種を超えるSNPを同時にタイピングするキットが市販されている。われわれは500K Human Mapping Array Setを用いる大規模なSNP解析システムを構築し、いくつかの多因子疾患についてゲノムワイド関連分析を実施している。その一例としてナルコレプシーの疾患感受性遺伝子の探索研究を紹介する。

## 0 技術原理

500K Human Mapping Array Set (以下、500K Array Set) は、制限酵素によるゲノムDNAの断片化とマイクロアレイによるタイピングの手法に改良を加えることにより、大規模なタイピングを行える手法として確立された<sup>8)</sup>。解析対象となるSNPは、公共のSNPデータベースおよびPerlegen社に登録されている約220万種のSNPから遺伝学的情報量が最大化されるように、また連鎖不平衡(LD)やHapMapプロジェクトからの情報も考慮して選択された約50万種

のSNPである。

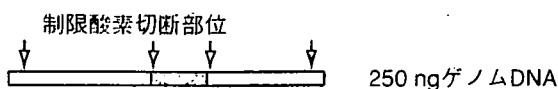
500K Array SetによるSNPタイピングは、ゲノムの複雑さを低減しマイクロアレイへのハイブリダイゼーション効率を上げるための酵素反応ステップと、洗浄・染色装置およびマイクロアレイ用スキャナーを用いた検出ステップに分けることができる(図1)。50万種のSNPタイピングは、2種類の制限酵素(*Sty I*, *Nsp I*)を用いてそれぞれ約25万種のSNPを独立にタイピングすることで実現される。制限酵素によるゲノムDNAの断片化を行った後、断片化されたゲノムDNAの両末端にアダプター配列をライゲーション反応により付加する。アダプター配列は、続くPCRで使用されるプライマーと相同な配列をもち、また制限酵素認識配列を突出端としても二本鎖DNAである。2種類の制限酵素(*Sty I*, *Nsp I*)のそれぞれに対して用意されるアダプター配列は、制限酵素認識配列を除いて共通の配列をもっているため共通のプライマーを使用してPCRを行うことができる。PCRでは、目的の長さをもったゲノムDNA断片(200~1,100 bp)だけが選択的に増幅される。ここまでの酵素反応により、もともと30億塩基対のゲノムDNAが5億塩基対程度のPCR混合産物となる。マイクロアレイへの効率的なハイブリダイゼーションには、ゲノムの複雑さを低減することが大きな役割を果たすと考えられている<sup>10) 11)</sup>。続いて、PCR産物の精製を行った後、DNase I制限酵素によりPCR産物の断片化を行う。断片化されたPCR産物は平均長で180 bp以下となる。マイクロアレイへの効率的なハイブリダイゼーションには、ゲノムの複雑さを低減することに加えてPCR産物の断片化が重要になる。最後にterminal deoxynucleotidyl transferase 酵素反応により、断片化されたPCR産物の末端にビオチンを導入する。

続いて、専用のマイクロアレイを用いてハイブリダイゼーションを行う。マイクロアレイには解析対象となる各SNPに対して合計24本のプローブが用意されている。プローブは25塩基長のオリゴDNAで、SNP部位を含む塩基配列をもっている。2種類のアレルに対して完全に相補的な塩基配列をもつプローブ(PMプローブ)と1塩基のミスマッチを含むプローブ(MMプローブ)を用意し、4種類のプローブを1組のプローブセットとしている。SNP部位を25塩基長のプローブの中心に置いたプローブセットを基本として、SNP

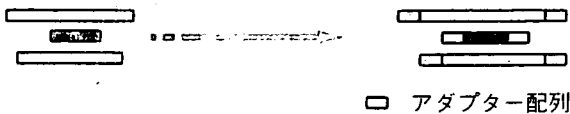
### ※1 ケース・コントロール関連分析

ある疾患に罹っている患者群(ケース)と健常者群(コントロール)とで遺伝子・ゲノム多型の頻度に差があるかどうかを検定することにより、疾患関連遺伝子を探索するための統計遺伝学的方法。

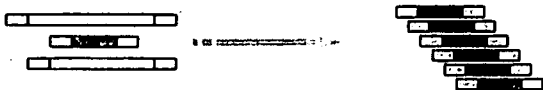
①制限酵素による断片化 (約3時間)



②ライゲーション (約4時間)

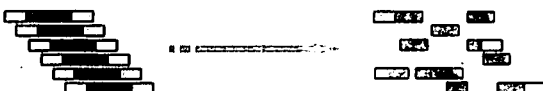


③PCR (約2時間)

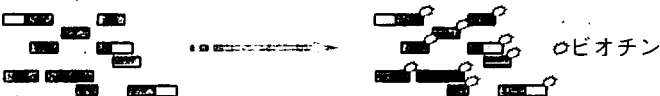


④PCR産物精製 (約2時間)

⑤断片化 (約1.5時間)



⑥ラベリング (約4時間)



⑦ハイブリダイゼーション (約16時間)

⑧アレイの洗浄・染色 (約2時間/run)

⑨スキャンニング (35分/Chip)

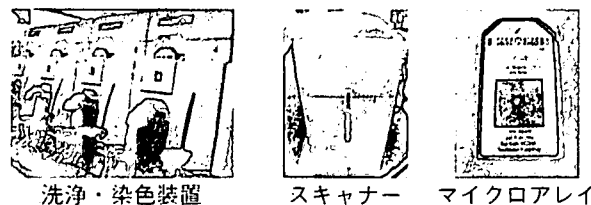


図1 500K Human Mapping Array SetによるSNPタイピングの原理

制限酵素による断片化からラベリングまでの酵素反応で得られた産物を洗浄・染色装置およびマイクロアレイ用スキャナーで検出することにより、約50万種のSNPのタイピングを行う

部位を中心から4塩基上流(+4)にずらしたプローブセットから4塩基下流(-4)にずらしたプローブセットまで7組のプローブセット(-4, -2, -1, 0, +1, +3, +4)の中から3組のプローブセットを選択する。3組のプローブセットはゲノムDNAの両鎖に対して用意されているので、合計6組のプローブセットが各SNPに対して用意されている。また、遺伝学的に重要だとされる約52,000 SNPsに関してはプローブセットを合計10組とし、計40本のプローブを用意している。すべてのプローブセットからのPMプローブとMMプローブのシグナル強度差を検出することで遺伝子型の判定を行うことができる。

マイクロアレイへのハイブリダイゼーションが終了した後、洗浄・染色装置を用いてマイクロアレイの洗浄および蛍光染色を行う。蛍光染色は、蛍光分子で標識されたストレプトアビジンが、前述のビオチン導入されたPCR断片に結合することにより行われる。また、洗浄・染色装置内ではビオチン修飾された抗スト

レプトアビジン抗体を用いてシグナルの増強が行われる。最後に蛍光染色されたマイクロアレイを専用のスキャナーで画像データとして読み取り、続いて専用の画像解析ソフトウェアを用いて各SNPの遺伝子型を決定する。

## ② システム構築

### 1) ハードウェアの整備

500K Array SetによるSNPタイピングを効率的に行うために、環境、装置を整備し、作業マニュアルを作成した。まず、ゲノムDNAへのPCR産物のコンタミネーションを防ぐために、試料調製室とSNP解析室を設けた。試料調製室にはゲノムDNAを保管し、PCR以前の酵素反応を行うのに必要な装置(サーマルサイクラーなど)を用意した。制限酵素による断片化からPCRの反応溶液の調製までは試料調製室で行い、PCR以降の酵素反応はSNP解析室で行った。また、3台の洗浄・染色装置を用意し、1回のランで計

12枚のマイクロアレイを洗浄・染色することができるようにした。すべてのマイクロアレイはバーコードで管理され、洗浄・染色が終了したマイクロアレイはオートローダー付きのマイクロアレイ用スキャナーに装填され画像データが読み込まれる。オートローダー付きのマイクロアレイ用スキャナーは計64枚のマイクロアレイを装填することができ、バーコードを参照しながらすべてのマイクロアレイの画像データを自動的に読み込むことができる。

SNPタイピング作業のルーチン化にあたって、制限酵素による断片化からラベリングまでの5つの酵素反応ステップで使用するすべてのマイクロタイタープレートをバーコードで管理する(図2)。また、1枚のマイクロタイタープレートで32検体分の酵素反応を行うこととし、制限酵素による断片化で使用するマイクロタイタープレートのウェル位置をサンプルと対応させることでサンプルのID化を行った。制限酵素による断片化以降の酵素反応で使用するマイクロタイタープレートでもレイアウトを変えずに酵素反応を行うことで、ウェル位置をサンプルIDとして解析結果を得ることができる。また、酵素反応の各工程を管理するためにチェックシートを作成し、反応工程の進行を随時チェックシートで確認しながら進める。PCRおよび断片化の酵素反応の後にはアガロースゲル電気泳動を行い、PCR産物および断片化産物の平均長がそれぞれ200~1,100 bp, 180 bp以下となっていることを確認する。加えて、同一のマイクロプレート上で酵素反応を行った32検体のうちから4検体だけを先行してハイブリダイゼーションを行い、SNPコール率に問題がないことを確認した後で残り28検体のハイブリダイゼーションを行った。28検体のハイブリダイゼーションを行う際に、次のマイクロタイタープレートから4検体を加えて合計32検体のハイブリダイゼーションを順次行っていくこととした。

## 2) ソフトウェアの開発

500K Array SetによるSNPタイピングではGeneChip® Operating Software (GCOS) とGeneChip® Genotyping Analysis Software (GTYPE) という2種類のソフトウェア(ともにAffymetrix社)を使用する。GCOSソフトウェアは洗浄・染色装置およびマイクロアレイ用スキャナーを操作する際に使用し、またGTYPEソフトウェアはマイクロアレイの画像デー

タから遺伝子型を判定する際に使用する。GTYPEソフトウェアで決定された約25万種のSNPの遺伝子型は、Sty I, Nsp Iごとにテキストファイルとして転送することができる。

われわれは500K Array SetによるSNPタイピングから得られる約50万SNPsの遺伝子型情報を用いてケース・コントロール関連分析を行うためのソフトウェアを開発した。ケース・コントロール関連分析をするにあたって、Sty IおよびNsp Iごとにまとめられた約25万SNPsの遺伝子型データを検体ごとに統合し、さらに検体をケース群およびコントロール群に分けて新たなテキストファイルとして作成する機能をソフトウェアに加えた。続いて、作成したケース群およびコントロール群の解析結果のテキストファイルを使ってケース・コントロール関連解析を行った。この際、各コントロール群における各遺伝子型の観察数からも、ハーディー・ワインベルク平衡<sup>※2</sup>の検定を行うこととした。ケース・コントロール関連分析の結果はレポートファイルとしてまとめられ、専用のビューアーを用いて表示することができる。

## 3 ナルコレプシー感受性領域のゲノムワイド探索

われわれは上に述べた大規模SNPタイピングシステムを用いて、文部科学省科学研究費特定領域研究「基盤ゲノム」におけるSNPタイピングセンターとして、数種の疾患のゲノムワイド関連分析を実施しており、すでに2種の疾患については約200名ずつの患者試料と約200名の健常者試料の解析を終了している。

またわれわれは睡眠障害の1つナルコレプシーの感受性・抵抗性遺伝子をゲノムワイド関連分析法によって探索している。すでに2万3千種のマイクロサテライト多型を用いたゲノムワイド関連解析を行い、11カ所の候補領域を検出するとともに、その1つから新たな疾患抵抗性遺伝子を同定した<sup>12)</sup>。現在、他の候補領域についても詳細な解析を行っているが、これと平行して、新たに50万種のSNPsを用いたゲノムワイド関

### ※2 ハーディー・ワインベルク平衡

自然淘汰が働かず、突然変異によって新たな対立遺伝子が生じず、また移住や混血などが起こらない十分に大きな規模の集団においては、対立遺伝子の頻度は世代を経ても変化しないという集団遺伝学の基本的法則。

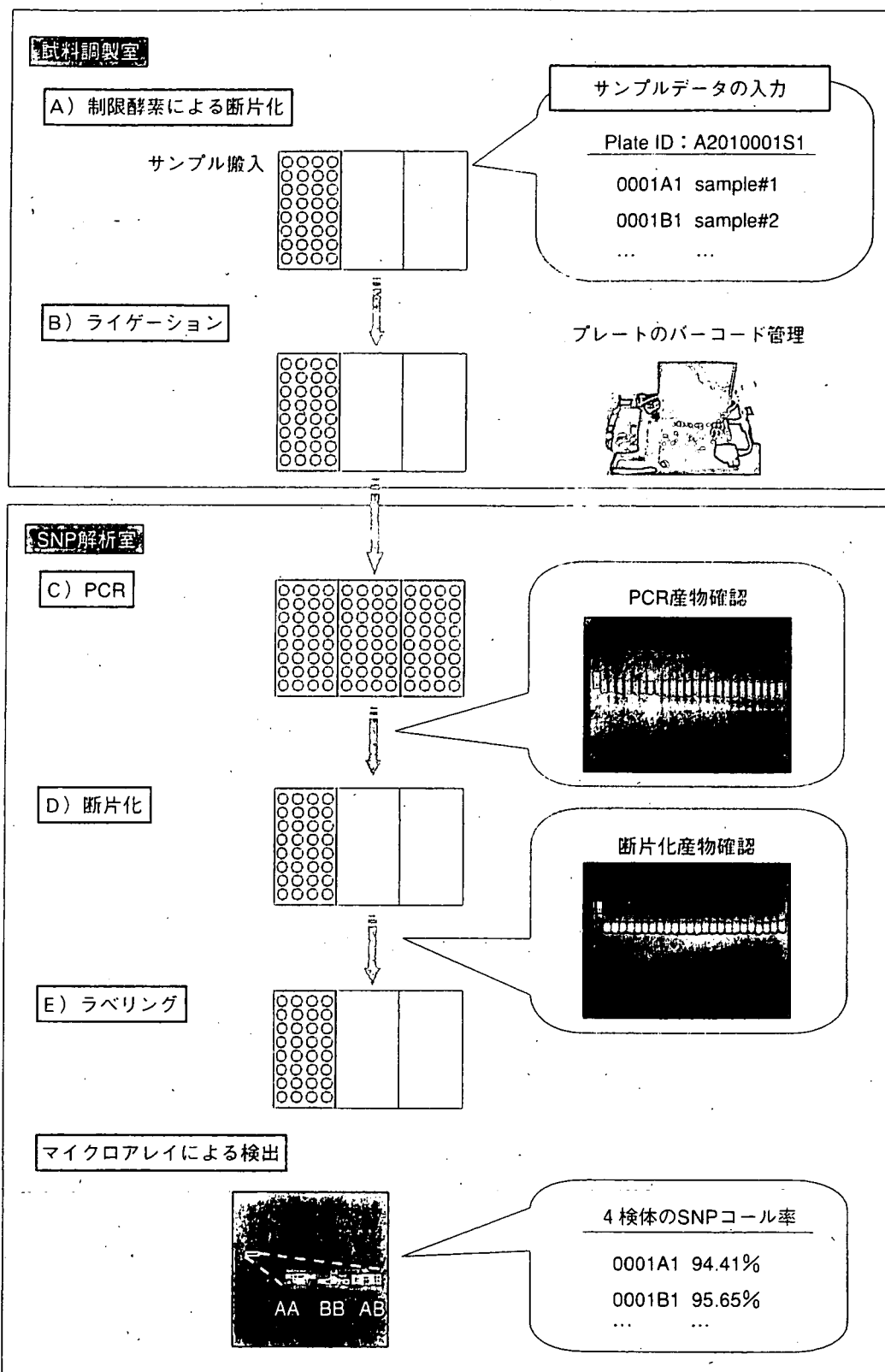


図2 SNPタイピングシステムの構築

500K Human Mapping Array Setを用いたSNPタイピングを効率的に行うためのシステム環境を構築し、作業マニュアルを作成した。96ウェルマイクロタイタープレートを使用して32検体ずつ解析を行う



表1 50万SNPsによるヒトナルコレプシーのゲノムワイド関連解析：関連SNP数の分布

有意水準	SNP数
$p < 0.0001$	214
$p < 0.001$	631
$p < 0.01$	3,665
$p < 0.05$	15,443
解析SNP総数	335,811

連分析も開始している。すでにタイピングおよび統計解析を終了した110名の患者試料と200名の健常者試料のデータから得られた関連SNPsの数の分布を表1に示す。call rate (>90%) およびハーディ・ワインベルク平衡からのずれ ( $p > 0.001$ ) に基づいて選別された約33万6千種のSNPsのうち、 $p < 0.0001$ の関連を示したSNPsが約200種検出された。なお、この解析には従来の遺伝子型判定ソフト (GTYPE4.0) を用いたデータを使用している。現在、新しい判定ソフト (GTYPE4.1) によってcall rateが向上していることから、より多くのSNPsについて統計解析することが可能になっている。ヒトのナルコレプシーについては、すでに確立した感受性遺伝子として6番染色体上の *HLA-DQB1* 遺伝子が知られている。図3は今回の解

析から *HLA* 遺伝子領域について得られた結果であるが、予想通り *HLA-DQB1* 遺伝子近傍をピークとする強い関連が認められた。現在われわれは、解析規模を2倍に拡大して新たなナルコレプシー感受性・抵抗性候補領域を検出している。

## おわりに

数十万種以上のSNPを一挙にタイピングできる技術の実用化によって、従来は存在しなかった広範かつ詳細なヒトゲノム多型情報が得られる時代となった。このような情報は、疾患遺伝子探索研究のみならず、人類の進化や人類集団の歴史を解明する糸口を提供し、ヒトゲノム多様性に関連するさまざまな研究分野に画期的なインパクトを及ぼすことは疑いない。

しかしながら同時に、われわれはまだ得られる膨大な多型情報を十分に活用できるノウハウをもっていないことも指摘しておきたい。500K Array SetによるSNPタイピングで得られる1検体当たりのファイルデータのサイズは約2 Gbであるため、何百、何千検体のデータを保管し、必要な時に取り出して解析するためのコンピュータ環境を整備することは容易ではない。また、われわれの統計解析ソフトウェアはおおのこのSNPについて関連分析できるものの、まだSNPハプロタイプについて関連分析することはできない。市販

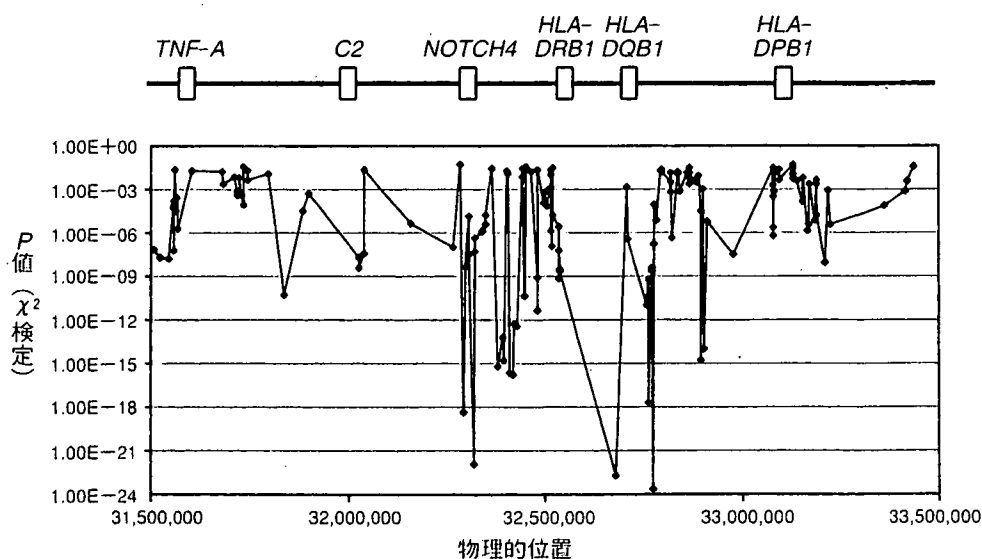


図3 ヒトナルコレプシーのゲノムワイド関連解析から *HLA-DQB1*, *HLA-DRB1* 遺伝子近傍領域におけるSNP関連マッピングによって強い疾患関連が検出された

のソフトウェアにも、限定した領域でハプロタイプ関連分析できるものはあるものの、ゲノム全域にわたって一挙に分析できるものはない。さらに、多数の検体について得られた50万SNPsデータから、これまで全く知られていなかった新しい遺伝子-遺伝子相互作用が見出される可能性がある。しかし残念ながら、従来の統計的手法や計算アルゴリズムでは、このように膨大なデータを実用的に処理できない。このように、ゲノムワイド多型解析情報はバイオインフォマティクスに関わるさまざまな研究者にとって挑戦に値する多くの課題を提供してくれるとともに、その達成によって従来にはない実り豊かな成果をもたらしてくれるに違いない。

## 文献

- 1) Ohashi, J. & Tokunaga, K. : J. Hum. Genet., 46 : 478-482, 2001
- 2) 徳永勝士 : 「人類遺伝学ノート」, 南山堂 (印刷中)
- 3) Kruglyak, L. & Nickerson, D. A. : Nat. Genet., 27 : 234-236, 2001

- 4) Syvänen, A. -C. : Nat. Rev. Genet., 2 : 930-942, 2001
- 5) Kwok, P. -Y. & Chen, X. : Curr. Issues Mol. Biol., 5 : 43-60, 2003
- 6) Nishida, N. et al. : Anal. Biochem., 346 : 281-288, 2005
- 7) Rachagani, S. et al. : BMC Genetics, 7 : 31, 2006
- 8) Matsuzaki, H. et al. : Genome Research, 14 : 414-425, 2004
- 9) Oliphant, A. et al. : BioTechniques, 32 : S56-S61, 2002
- 10) Grant, S. F. et al. : Nucleic Acids Res., 30 : e125, 2002
- 11) Jordan, B. et al. : Proc. Natl. Acad. Sci. USA, 99 : 2942-2947, 2002
- 12) Kawashima, M. et al. : Am. J. Hum. Genet., 79 : 252-263, 2006

## <著者プロフィール>

西田奈央 : 東京大学大学院総合文化研究科で博士号を取得後、東京大学大学院医学系研究科人類遺伝学分野 (徳永勝士教授) にて研究員として従事、研究課題は遺伝子多型解析手法の開発。

徳永勝士 : 東京大学理学部、同医学部附属病院、日本赤十字中央血液センターを経て、1995年より東京大学大学院医学系研究科教授。研究課題はヒトゲノム多様性および複合疾患の遺伝要因とその機能。

## Further development of multiplex single nucleotide polymorphism typing method, the DigiTag2 assay

Nao Nishida <sup>a,\*</sup>, Tetsuya Tanabe <sup>b</sup>, Miwa Takasu <sup>a</sup>, Akira Suyama <sup>c</sup>, Katsushi Tokunaga <sup>a</sup>

<sup>a</sup> Department of Human Genetics, Graduate School of Medicine, University of Tokyo, Bunkyo-ku, Tokyo 113-0033, Japan

<sup>b</sup> Bio Business Division, Olympus Corporation, Hachioji, Tokyo 192-8512, Japan

<sup>c</sup> Department of Life Sciences, Graduate School of Arts and Sciences, University of Tokyo, Meguro-ku, Tokyo 153-8902, Japan

Received 21 December 2006

Available online 13 February 2007

### Abstract

A number of single nucleotide polymorphisms (SNPs) are considered to be candidate susceptibility or resistance genetic factors for multifactorial disease. Genome-wide searches for disease susceptibility regions followed by high-resolution mapping of primary genes require cost-effective and highly reliable technology. To accomplish successful and low-cost typing for candidate SNPs, new technologies must be developed. We previously reported a multiplex SNP typing method, designated the DigiTag assay, that has the potential to analyze nearly any SNP with high accuracy and reproducibility. However, the DigiTag assay requires multiple washing steps in manipulation and uses genotyping probes modified with biotin for each target SNP. Here we describe the next version of the assay, DigiTag2, which works with simple protocols and uses unmodified genotyping probes. We investigated the feasibility of the DigiTag2 assay by genotyping 96 target SNPs spanning a 610-kb region of human chromosome 5. The DigiTag2 assay is suitable for genotyping an intermediate number of SNPs (tens to hundreds of sites) with a high conversion rate (> 90%), high accuracy, and low cost.

© 2007 Elsevier Inc. All rights reserved.

**Keywords:** Multiplex genotyping; SNPs; Mutation; Oligonucleotide ligation assay

As a consequence of the Human Genome Project and single nucleotide polymorphism (SNP)<sup>1</sup> discovery projects, several million SNPs have been uploaded onto public SNP databases. It is estimated that there are 5 million SNPs with a greater than 10% minor allele frequency and 11 million SNPs with a greater than 1% minor allele frequency in the human genome [1]. Among these SNPs, many are candidate susceptibility or resistance genetic factors for multifactorial diseases and have been identified based on linkage analysis

in families or association analysis with unrelated patients (cases) and healthy controls [2–6]. Large-scale case-control analyses using a dense set of SNP markers across the human genome have revealed associations between various diseases and SNPs with the highest detection power [7–9].

During recent years, genome-wide association studies using SNP markers have attempted to search for susceptibility and/or resistance genes by using emerging genome-wide SNP typing technologies such as Affymetrix GeneChip arrays and Illumina BeadArray genotyping technology [10–13]. These genome-wide SNP typing technologies would detect candidate regions, including susceptibility or resistance genes. However, to identify primary SNPs or genes, it is necessary to perform association analysis using an intermediate number of SNPs (tens to hundreds of sites) located within the candidate regions. Currently, there are a variety of SNP genotyping methods that are suitable for genotyping large numbers of samples for a modest number of SNPs such as 5' exonuclease

\* Corresponding author. Fax: +81 3 5802 8619.

E-mail address: [nishida-75@umin.ac.jp](mailto:nishida-75@umin.ac.jp) (N. Nishida).

<sup>1</sup> Abbreviations used: SNP, single nucleotide polymorphism; MALDI-TOF MS, matrix-assisted laser desorption/ionization time-of-flight mass spectrometry; ED, end digit; D1, first digit; PCR, polymerase chain reaction; dNTP, deoxynucleoside triphosphate; ATP, adenosine triphosphate; DTT, dithiothreitol; NAD, nicotinamide adenosine dinucleotide; EDTA, ethylenediaminetetraacetic acid; Cy3-ED-1, Cy3-labeled ED-1; Cy5-ED-2, Cy5-labeled ED-2; SDS, sodium dodecyl sulfate; DCN, DNA coded number.

fluorescence-based assay (TaqMan) [14], pyrosequencing [15], single-base extension [16], matrix-assisted laser desorption/ionization time-of-flight mass spectrometry (MALDI-TOF MS) [17,18], and SNPlex assay [19]. However, many applications need to select relevant SNPs for their assay by *in silico* assay design, and some candidate SNPs are then excluded from investigation. Moreover, it is difficult or impossible for some assays to perform multiplex SNP genotyping.

To accomplish successful SNP typing for all candidate SNPs at low cost, new technologies must be developed. We previously reported a multiplex SNP typing method, designated the DigiTag assay, that has a high conversion rate (>90%) and reliable accuracy [20]. However, the DigiTag assay requires improvement with regard to simplifying assay protocols and reducing assay cost. In this study, we developed the DigiTag2 assay, which has simplified assay protocols, and performed typing for 96 SNP sites located in a 610-kb region on human chromosome 5 using 48 individual genomic DNA samples.

## Materials and methods

### DNA samples

Genomic DNA samples from 48 unrelated healthy donors were obtained from the Japan Health Science Foundation (Osaka, Japan). All donors provided written informed consent, and samples were anonymized. For each sample, 1 µg of purified genomic DNA was dissolved in 20 µl of TE buffer (pH 8.0, Wako, Osaka, Japan) for use and was stored at -20 °C.

### End digits and first digits

We designed the end digits (EDs) and first digits (D1s) to be 23-mer oligonucleotides and attached the EDs and D1s to 5' query probes and 3' query probes, respectively. We prepared two EDs (ED-1 and ED-2) for two alleles at each SNP. All EDs and D1s are used for the priming site in the labeling step, and D1s are also used as probes that are attached to DNA microarray in the detection step. The EDs and D1s have the following properties: (i) uniform melting temperature ( $58.8 \pm 1.0$  °C) and length, (ii) specific hybridization only to complementary EDs and D1s, (iii) minimal interaction with other EDs and D1s, and (iv) no formation of secondary structures [21]. These properties ensure uniform polymerase chain reaction (PCR) efficiency, even if all of the EDs and D1s are used in multiplex PCR. Furthermore, precise hybridization on DNA microarray is possible using a set of D1s with high reproducibility. Sequence information for EDs and D1s is listed in Supplementary Table 1.

### Multiplex PCR from sample DNA

We designed multiplex PCR primers for each of the 96 SNP sites to have relatively long length (average length 40-

mer) and to give PCR products of between 181 and 798 bp (average length 527 bp). Sequence information for the multiplex PCR primers is listed in Supplementary Table 2.

We performed multiplex PCR using a two-step protocol (denature and extension steps) with a 6-min extension step using specifically designed primer pairs. Multiplex PCR was performed with 2.5 µl genomic DNA and 250 fmol of each primer for 96 SNP sites in 10 µl of 2× Qiagen Multiplex PCR Master Mix containing HotStarTaq DNA polymerase, multiplex PCR buffer and deoxynucleoside triphosphate (dNTP) mix (Qiagen Multiplex PCR Kit, Qiagen, Valencia, CA, USA). Cycling was performed using a Bio-Rad PTC-200 Peltier thermal cycler (Bio-Rad, Hercules, CA, USA) as follows: 95 °C for 15 min, followed by 40 cycles of 95 °C for 30 s and 68 °C for 6 min. When necessary, fragment length of the 96 PCR products was confirmed by capillary electrophoresis (Agilent 2100 Bioanalyzer, Agilent, Palo Alto, CA, USA) to evaluate PCR efficiency.

### Encoding reaction

We performed multiplex oligonucleotide ligation assay using the multiplex PCR products as targets. For 96-plex oligonucleotide ligation assay, we prepared mismatch-induced 5' query probes for 91 target SNPs and perfect match 5' query probes for 5 target SNPs (SNP 7, SNP 9, SNP 18, SNP 49, and SNP 93). The assignment of D1s to the SNPs analyzed in this study and sequence information for the probes are listed in Supplementary Table 3.

Prior to the encoding reaction, 96 unmodified 3' query probes were simultaneously phosphorylated at the 5' end in 40 µl of 1× protruding end kinase buffer containing 30 mM adenosine triphosphate (ATP), 40 U polynucleotide kinase, and 4 pmol of 3' query probes for 96 SNP sites (Kination Kit, Toyobo, Osaka, Japan). The reaction mixture was incubated for 30 min at 37 °C and for 3 min at 95 °C using a Bio-Rad PTC-200 Peltier thermal cycler. The encoding reaction was prepared by mixing 1 µl of multiplex PCR products in 15 µl of *Taq* DNA ligase buffer containing 20 mM Tris-HCl (pH 7.6), 25 mM potassium acetate, 10 mM magnesium acetate, 10 mM dithiothreitol (DTT), 1 mM nicotinamide adenosine dinucleotide (NAD), and 0.1% Triton X-100 (New England Biolabs, Beverly, MA, USA) with 10 fmol of probes (192 5' query probes and 96 phosphorylated 3' query probes) and 10 U *Taq* DNA ligase. All components of the encoding reaction were mixed on ice. The encoding reaction initially was held at 95 °C for 5 min, followed by 58 °C for 15 min using a Bio-Rad PTC-200 Peltier thermal cycler. The reaction was stopped by holding the temperature at 10 °C.

### Labeling reaction

For the labeling reaction, 6 µl of ligation products was directly mixed in 12 µl of *Ex Taq* buffer containing 20 mM Tris-HCl (pH 8.0), 100 mM KCl, 0.1 mM ethylenediamine-tetraacetic acid (EDTA), 1 mM DTT, 0.5% Tween 20, 0.5%